

# NAVAL POSTGRADUATE SCHOOL MONTEREY, CALIFORNIA



## THESIS

**AN ANALYSIS OF THE SYNOPTIC AND  
MESOSCALE FORCING OF THE 08/09 MARCH  
1992 STORMFEST MESOSCALE CONVECTIVE  
SYSTEM**

by

Raymond M. Robichaud Jr.

March, 1995

Thesis Advisor:

Wendell Nuss

Approved for public release; distribution is unlimited.

19960401 076

DTIC QUALITY INSPECTED 1

REPORT DOCUMENTATION PAGE			Form Approved OMB No. 0704-0188	
Public reporting burden for this collection of information is estimated to average 1 hour per response, including the time for reviewing instruction, searching existing data sources, gathering and maintaining the data needed, and completing and reviewing the collection of information. Send comments regarding this burden estimate or any other aspect of this collection of information, including suggestions for reducing this burden, to Washington Headquarters Services, Directorate for Information Operations and Reports, 1215 Jefferson Davis Highway, Suite 1204, Arlington, VA 22202-4302, and to the Office of Management and Budget, Paperwork Reduction Project (0704-0188) Washington DC 20503.				
1. AGENCY USE ONLY (Leave blank)		2. REPORT DATE March 1995		3. REPORT TYPE AND DATES COVERED Master's Thesis
4. AN ANALYSIS OF THE SYNOPTIC AND MESOSCALE FORCING OF THE 08/09 MARCH 1992 STORMFEST MESOSCALE CONVECTIVE SYSTEM			5. FUNDING NUMBERS	
6. AUTHOR(S) *Raymond M. Robichaud Jr.				
7. PERFORMING ORGANIZATION NAME(S) AND ADDRESS(ES) Naval Postgraduate School Monterey CA 93943-5000			8. PERFORMING ORGANIZATION REPORT NUMBER	
9. SPONSORING/MONITORING AGENCY NAME(S) AND ADDRESS(ES)			10. SPONSORING/MONITORING AGENCY REPORT NUMBER	
11. SUPPLEMENTARY NOTES The views expressed in this thesis are those of the author and do not reflect the official policy or position of the Department of Defense or the U.S. Government.				
12a. DISTRIBUTION/AVAILABILITY STATEMENT Approved for public release; distribution is unlimited.			12b. DISTRIBUTION CODE	
13. ABSTRACT (maximum 200 words) A severe mesoscale convective system (MCS) developed in northeast Texas and southern Oklahoma during STORMFEST in 1992. The MCS, associated with a bulging dryline, produced five tornadoes, widespread flashflooding, large hail and damaging winds. An analysis of the root causes of this convective system was conducted using the coarse gridded Global Data Assimilation (GDAS) Final Analysis fields. This analysis is conducted to determine if the atmospheric processes that produce such severe convection are resolveable in coarse gridded data. Bulging dryline convection is associated with upper-level jet streaks which are synoptic-scale features. This research focusses on the interaction of the jet streak aloft, the dryline and an advancing cold front. Vertical motion associated with upper-tropospheric ageostrophic wind accelerations and motion along a cold frontal surface act together in producing severe convection along a bulging dryline. These forces are resolveable in the GDAS fields.				
14. SUBJECT TERMS *Mesoscale Convective System, Dryline, Squall Line.			15. NUMBER OF PAGES * 69	
			16. PRICE CODE	
17. SECURITY CLASSIFICATION OF REPORT Unclassified	18. SECURITY CLASSIFICATION OF THIS PAGE Unclassified	19. SECURITY CLASSIFICATION OF ABSTRACT Unclassified	20. LIMITATION OF ABSTRACT UL	

NSN 7540-01-280-5500

Standard Form 298 (Rev. 2-89)

Prescribed by ANSI Std. Z39-18 298-102



Approved for public release; distribution is unlimited.

AN ANALYSIS OF THE SYNOPTIC AND MESOSCALE FORCING OF  
THE 08/09 MARCH 1992 STORMFEST MESOSCALE CONVECTIVE  
SYSTEM

Raymond M. Robichaud Jr.  
Lieutenant Commander, United States Navy  
B.S., U.S. Naval Academy, 1982

Submitted in partial fulfillment  
of the requirements for the degree of

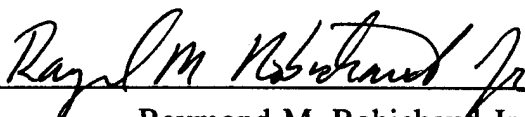
MASTER OF SCIENCE IN METEOROLOGY AND PHYSICAL  
OCEANOGRAPHY

from the

NAVAL POSTGRADUATE SCHOOL

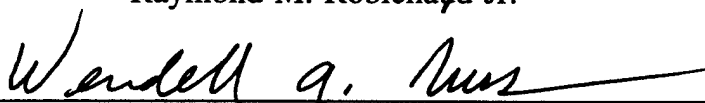
March, 1995

Author:



Raymond M. Robichaud Jr.

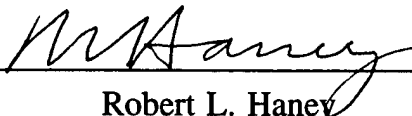
Approved by:



Wendell Nuss, Thesis Advisor



Teddy Holt, Second Reader



Robert L. Haney  
Department of Meteorology



## ABSTRACT

A severe mesoscale convective system (MCS) developed in northeast Texas and southern Oklahoma during STORMFEST in 1992. The MCS, associated with a bulging dryline, produced five tornadoes, widespread flashflooding, large hail and damaging winds. An analysis of the root causes of this convective system was conducted using the coarse gridded Global Data Assimilation (GDAS) Final Analysis fields. This analysis is conducted to determine if the atmospheric processes that produce such severe convection are resolveable in coarse gridded data. Bulging dryline convection is associated with upper-level jet streaks which are synoptic-scale features. This research focusses on the interaction of the jet streak aloft, the dryline and an advancing cold front. Vertical motion associated with upper-tropospheric ageostrophic wind accelerations and motion along a cold frontal surface act together in producing severe convection along a bulging dryline. These forces are resolveable in the GDAS fields.



## TABLE OF CONTENTS

I.	INTRODUCTION . . . . .	1
A.	STORMFEST . . . . .	1
B.	EVOLUTION OF THE CONVECTION . . . . .	1
C.	DATA SETS . . . . .	2
D.	EVALUATION OF ANALYSIS DATA . . . . .	2
E.	OBJECTIVE OF RESEARCH . . . . .	3
II.	DRYLINES AND CONVECTION INITIATION . . . . .	5
A.	A BASIC DESCRIPTION OF DRYLINES . . . . .	5
B.	DRYLINE CONTRIBUTION TO CONVECTIVE INSTABILITY . . . . .	5
C.	CONVECTION INITIATION . . . . .	6
III.	THE ROLE OF LOW-LEVEL WIND SHEAR . . . . .	9
A.	LOW-LEVEL WIND SHEAR (LLWS) AND SQUALL LINES . . . . .	9
1.	Squall Line Environment . . . . .	9
2.	Supercells versus Ordinary Cells . . . . .	10
B.	THUNDERSTORM SIMULATIONS . . . . .	11
1.	Varying Shears . . . . .	11
2.	The Ideal Situation for Long-Lived, Severe Convection . . . . .	11
IV.	UPPER-LEVEL JET STREAKS AND VERTICAL CIRCULATIONS . . . . .	15
A.	JET STREAKS . . . . .	15
B.	JET STREAK INDUCED VERTICAL CIRCULATIONS . . . . .	15
V.	INITIALIZATION DATA/MODEL DESCRIPTION . . . . .	19
A.	ANALYSIS FIELDS . . . . .	19
1.	National Meteorological Center Gridded Analysis Fields . . . . .	19

2.	National Center for Atmospheric Research	
	(NCAR) Enhanced Data . . . . .	19
	a. Composite Surface Data . . . . .	19
	b. Data Networks . . . . .	19
B.	ANALYSIS SOFTWARE . . . . .	20
	1. Visual . . . . .	20
	2. NCAR Zeb Software . . . . .	20
VI.	PRE-CONVECTION ENVIRONMENT . . . . .	23
A.	SYNOPTIC FORCING . . . . .	23
	1. Overview . . . . .	23
	2. Atmospheric Stability Analysis . . . . .	25
	3. Surface and Lower-Tropospheric	
	Discussion . . . . .	26
	4. Upper-Level Jet Streak Analysis . . . . .	27
	5. Vertical Motion Discussion . . . . .	28
B.	MESOSCALE FORCING . . . . .	29
VII.	CONCLUSION . . . . .	51
VIII.	RECOMMENDATIONS . . . . .	53
	LIST OF REFERENCES . . . . .	55
	INITIAL DISTRIBUTION LIST . . . . .	57



## **ACKNOWLEDGEMENTS**

Thank you to my wonderful wife, Cindy, whose understanding and help made this a successful accomplishment.

## **I. INTRODUCTION**

### **A. STORMFEST**

The STORM Fronts Experiment Systems Test, hereafter referred to as STORMFEST, was designed with three objectives in mind: 1) investigation of the structures and evolution of fronts and associated mesoscale phenomena, 2) a research assessment of new operational and research meteorological instrumentation, facilities and composite observational networks, and 3) a study evaluating mesoscale prediction capabilities and limitations in active frontal regions. The experiment lasted 45 days from 1 February through 15 March 1992. Twenty Intensive Observation Periods (IOPs) ensured high temporal resolution in data collection (Cunning and Williams, 1993). A multitude of observational networks augmented by Portable Automated Mesonet (PAM) sites provided high spatial resolution for analysis and model initialization. The observational networks are described in section V-A.

The domain of the experiment covered a large portion of the Midwest. This area is indicated by the enclosed area on Fig. 1.1. This particular area was chosen due to existing observational networks and the anticipated frequency of frontal passages.

### **B. EVOLUTION OF THE CONVECTION**

A Mesoscale Convective System (MCS) was initiated along a dryline in northeast Texas and southwest Oklahoma during the middle to late afternoon of March 08, 1992. A very complex interaction of a cold front, a strong upper-level jet streak and the dryline contributed to very strong and deep convection. The area in which the MCS formed, southwest Oklahoma and north central Texas near Wichita Falls, will be referred to as the *genesis region*.

The first convective cells developed between 2100Z and 2200Z. Satellite imagery indicates that by 0000Z convection was developing along a great length of the dryline, with two very strong cells, possibly supercells, causing storm-related damage. This MCS produced 5 F1 and F0 tornadoes, baseball sized hail and 52 knot downburst winds in Texas. Flash flooding was also associated with this system. The flooding resulted in the closing of 50 roads in Titus county. The MCS lasted more than ten hours.

### **C. DATA SETS**

Much of the analysis of the pre-convection environment was done with the National Meteorological Center (NMC) Global Data Assimilation (GDAS) Final Analysis. This three-dimensional data set has a horizontal resolution of 2.5 by 2.5 degrees. GDAS data facilitated use of *Visual* (see section V.B.1) as the main display software package, and initialization of the Pennsylvania State University/National Center for Atmospheric Research (NCAR) Mesoscale Model version 5 (MM5).

Enhanced observational data collected by NCAR was available on a CD-ROM set provided by NCAR (see section V.A.2). The composite surface data was used for mesoscale analysis. Radar, skew-T and profiler data was also included on the CD-ROM. This data was crucial to the analysis as it allowed the evaluation of the true strength of the upper-level jet streak and low-level wind shear.

### **D. EVALUATION OF ANALYSIS DATA**

Analysis of the coarse NMC gridded data revealed the processes that were responsible for the severity of the convection (see Chapter VI). A convectively unstable environment was fueled by an advancing dryline and low-level jet. The potential instability was then released by a complex

interaction of the dryline, a surface cold front and an upper-level jet streak.

The NMC fields exposed these features; however, only analysis of the enhanced surface data and profiler data identified the intensity of the jet streak and low-level jet. Profiler data suggested that the jet streak was thirty per cent stronger than indicated in the gridded data. Analysis of the enhanced surface data also indicates that the convection was initiated as the cold front propagated into the dryline.

#### **E. OBJECTIVE OF RESEARCH**

The main objective of this research is to identify the physical atmospheric processes contributing to the severity of the convection. It was imperative to understand these processes to determine if they were resolvable in coarse resolution analyses fields. If severe convection of this type is forced by synoptic-scale features resolvable in readily available gridded fields, such as the NMC GDAS, then mesoscale models can be initialized with this data in an effort to predict severe convective events.



## **II. DRYLINES AND CONVECTION INITIATION**

### **A. A BASIC DESCRIPTION OF DRYLINES**

A dryline is basically a boundary separating two air masses of contrasting moisture content. This paper's description will concentrate on drylines in the lower Midwest of the United States.

The dryline boundary marks a zone separating the moist, northward-flowing Gulf of Mexico air from the much drier air advected into the southwest United States from the plateaus of Mexico. The moist layer is bounded on the west by the slopes of the Rockies. Consequently, the dryline is oriented as a rather north-south zone of strong moisture gradient. The slope of the terrain creates a situation where the western border of the moist layer is much more shallow than the eastern part of the layer. The shallow depth of the western part of the layer allows daily insolation and vertical turbulent mixing of heat and moisture to rapidly evaporate the moisture in the layer. This causes rapid eastward progression of the dryline during daylight hours.

During daylight hours, the dry air west of the dryline becomes very warm and dry, thereby intensifying the gradient. This diurnal variation gives the dryline better daytime definition. Also, regions at elevations higher than 500 m above sea level experience more intense drylines than lower areas (Schaefer, 1986).

### **B. DRYLINE CONTRIBUTION TO CONVECTIVE INSTABILITY**

In the vicinity of the dryline, very moist, low-level air near the surface underlies very dry and warmer air advected from the southwest. This creates a capping inversion or "lid" that inhibits free buoyancy, or convection. This allows the low-level air to moisten and warm throughout the day and

acquire very high potential temperature values. Throughout the day, continued warm, dry air advection aloft may also strengthen the cap. This may increase the severity of the convection.

According to McCarthy and Koch (1982), a dryline bulge is consistent with severe convection. A bulge may form if a middle to upper-level jet advects increased warm, dry air in a band the width of the bulge (Schaefer, 1986). Moisture convergence is maximized at the bulge. This is due to confluence of the southwesterly and southeasterly low-level airstreams. Once again, the moisture convergence allows the air below the capping inversion to attain very high virtual potential temperature values.

### **C. CONVECTION INITIATION**

A potentially unstable atmosphere requires some type of physical mechanism to release that instability. There are many mechanisms that can trigger instability along a dryline. Forced ascent associated with a transverse vertical circulation and upper-level jet streak, strong positive vorticity advection (PVA), and low-level underrunning are the primary mechanisms to be discussed here.

Upper-level jet streaks and short waves play significant roles in severe convective events. The divergence associated with the accelerations of the ageostrophic wind component and PVA aloft result in ascent that lifts the low-level air above the capping inversion. The positive buoyancy of the high  $\theta_e$  air produces violent convection.

Southerly near-surface flow, often aided by the low-level jet, may advect warm, moist air across the dryline and into an area where the capping inversion is not excessively strong. This is termed "underrunning." If the low-level air is

advected into an area where the surface air is warmer than the inversion air, then the instability is released in the form of severe convection.



### III. THE ROLE OF LOW-LEVEL WIND SHEAR

#### A. LOW-LEVEL WIND SHEAR (LLWS) AND SQUALL LINES

##### 1. Squall Line Environment

Thunderstorms are generally short-lived convective weather phenomena. They evolve in an environment of convective instability and progress from initiation through decay in an average of thirty minutes to an hour. They decay as the cool downdraft air propagates out ahead of the updraft and eliminates the source of moist, warm inflow air. Under certain conditions, the lifespan of a thunderstorm can be extended for hours. These long-lived thunderstorms are of two types: 1) individual supercell thunderstorms, or 2) ordinary cells being regenerated in some type of mesoscale convective system (MCS), (Rotunno et al., 1988). In either case, vertical wind shear is critical to the sustenance of long-lived, deep convection. LLWS, with respect to convection, is basically the vector difference between the surface wind and a level usually three kilometers above the ground.

The dynamics of the interaction of LLWS and the thunderstorm are very complex. As the vertical wind shear becomes stronger, the influence of the updraft on the sheared flow becomes critical to the organization of the convection. The essential physical mechanism responsible for this is the development of rotation on the flank of the updraft. If the LLWS extends through the mid-levels of the storm (~4-6 km), the rotation dynamically induces a pressure deficit that is strongest several kilometers above the ground. This produces a vertical pressure gradient that accelerates surface air upward. Supercells owe their existence to these dynamics (Weisman and Klemp, 1986).

## **2. Supercells versus Ordinary Cells**

Long-lived squall lines have been studied extensively, through evaluation of observational data and through numerical simulations. Long-lived squall lines of the two types, supercells and ordinary cells, evolve in unique environments.

Ordinary cell squall lines require a convectively unstable environment with strong low-level wind shear oriented normal to the developing line of thunderstorm cells to sustain itself. In Fig. 3.1a, taken from Rotunno et al. (1988), a typical ordinary cell in a no LLWS environment is depicted. It can be seen that the propagating cold surge cuts off the required inflow of warm, moist air. The cold surge is identified as a "cold pool" in the figure. The "cold pool" is a mesoscale mass of relatively cold air positioned behind the outflow boundary. This mass is produced by evaporative cooling associated with the rain-induced downdraft. Introducing moderate to strong LLWS as in 3.1b, the shear and mean flow maintain the updraft just ahead of the surface outflow forcing much longer-lived convection. Figure 3.1c indicates that in a no-shear environment, the thermal circulation along the outflow boundary inhibits new cell growth. In an environment with LLWS, however, as the outflow boundary propagates away into a moisture-rich region, the LLWS counteracts the thermal circulation along the outflow boundary and new convective updrafts are initiated in a cyclic fashion, (Fig. 3.1d).

Supercell squall lines evolve in a different environment. Rotunno et al. (1988) noted that in simulations with strong and deep vertical wind shear in which supercells evolved, the storms split and interacted, inhibiting sustained convection. However, in simulations with LLWS oriented at an angle of 45 degrees to the line, the splitting storms intensified without interacting. Fig. 3.2 depicts the orientation of the shear to the line of supercells and updraft motion.

## **B. THUNDERSTORM SIMULATIONS**

### **1. Varying Shears**

Weisman and Klemp (1984), hereafter referred to as WK, conducted a considerable number of experiments and simulations devoted entirely to the relationship between vertical wind shear and convective storm evolution. They have suggested a dichotomy of storm structure with multi-cellular systems associated with weaker LLWS, and supercell growth associated with deeper and stronger vertical wind shear. A further classification indicates that supercell storms form on the right flank of thunderstorms systems, whereas multi-cellular growth favors the left flank. If the wind vectors turn counterclockwise with height, as opposed to clockwise, then the situation is reversed.

WK also indicate that the dynamical forces responsible for the two types of storm structure are quite different. Multi-cellular growth is related to the convergence ahead of the propagating gust front. Supercell evolution is more related to the complex interaction of the updraft and the vertical wind shear profile. This interaction produces enhanced surface convergence due to the formation of a mesolow and a dynamically induced vertical pressure gradient.

The series of experiments conducted by WK were successful in identifying three modes of evolution in varying shears: 1) ordinary short-lived cells in weak shear, 2) multi-cellular systems associated with moderate shear, and 3) supercells with strong, deep shear.

### **2. The Ideal Situation for Long-Lived, Severe Convection**

The interaction of the outflow boundary and associated "cold pool" with the LLWS is the single most dominant factor in determining the structure and longevity of convection. The "optimal state" as described by Rotunno et al. (1988), is when the full potential of the instability is released. This

situation occurs when the strength of the cold pool circulation is perfectly balanced by the LLWS. In the situation when LLWS is dominated by the strength of the cold pool circulation, a long-lived state may occur. However, the updraft will become highly slanted. This produces weaker updrafts, but may result in long periods of precipitation. When the LLWS dominates the cold pool circulation, low-level inflow air is advected through the rainy downdraft region. The convergence along the outflow boundary is enough to maintain convection; however, the shear depletes the updraft cells of their convective vigor. This situation results in a long-lived line of very weak cells.

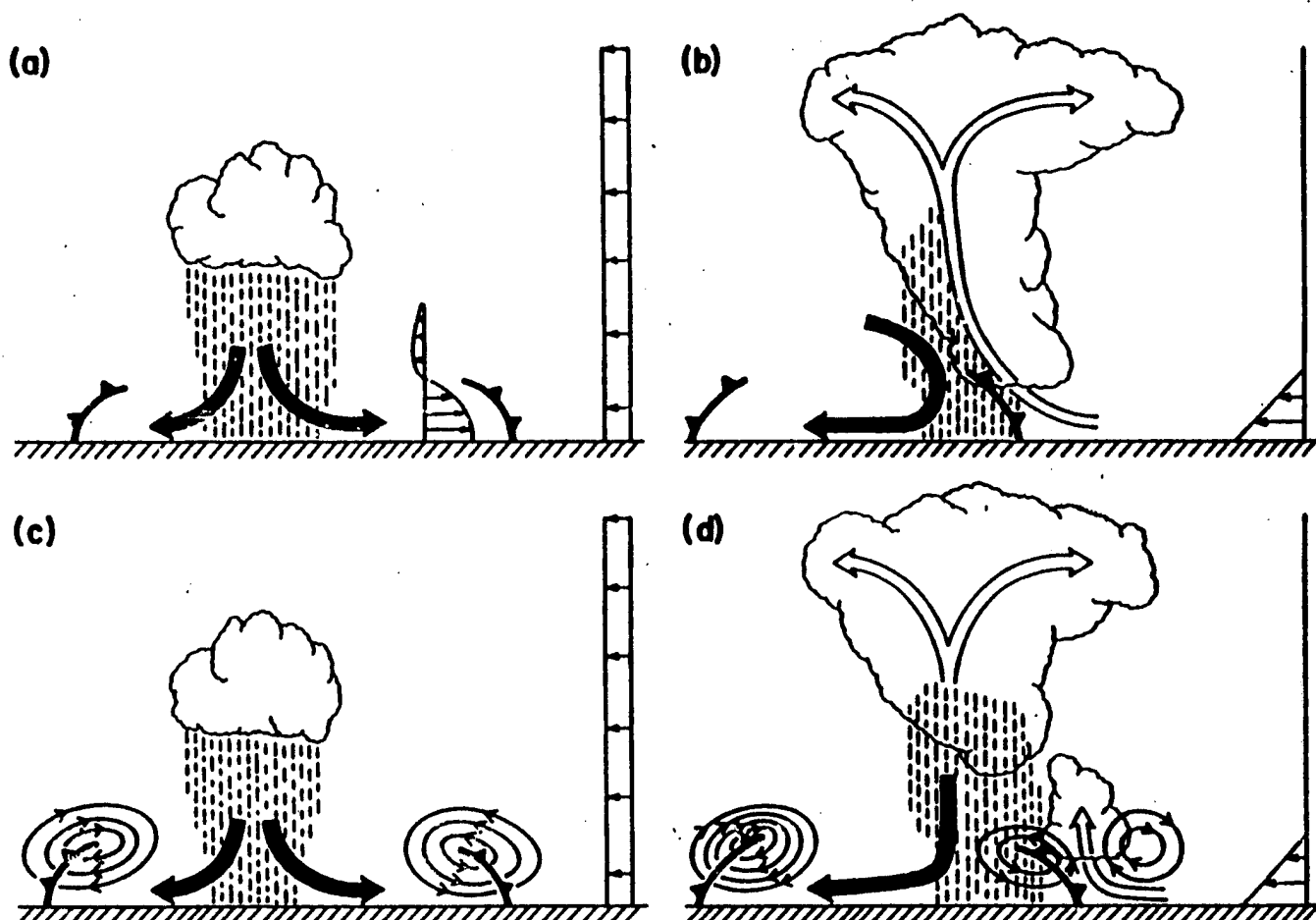


Fig. 3.1. Updraft response to LLWS and cold pool interaction. In (a), with no LLWS, the outflow boundary propagates away from the cloud and shear at the top of the cold pool dissipates new cells. In (b), with LLWS, the updraft remains just ahead of the outflow boundary producing a steady cell. In (c), without LLWS, the circulation of the spreading cold pool inhibits deep lifting and the triggering of new cells. In (d); with LLWS, the circulation of the cold pool counters the effect of the LLWS and promotes deep lifting and convergence, triggering new cells. (Adapted from Rotunno et al., 1988)

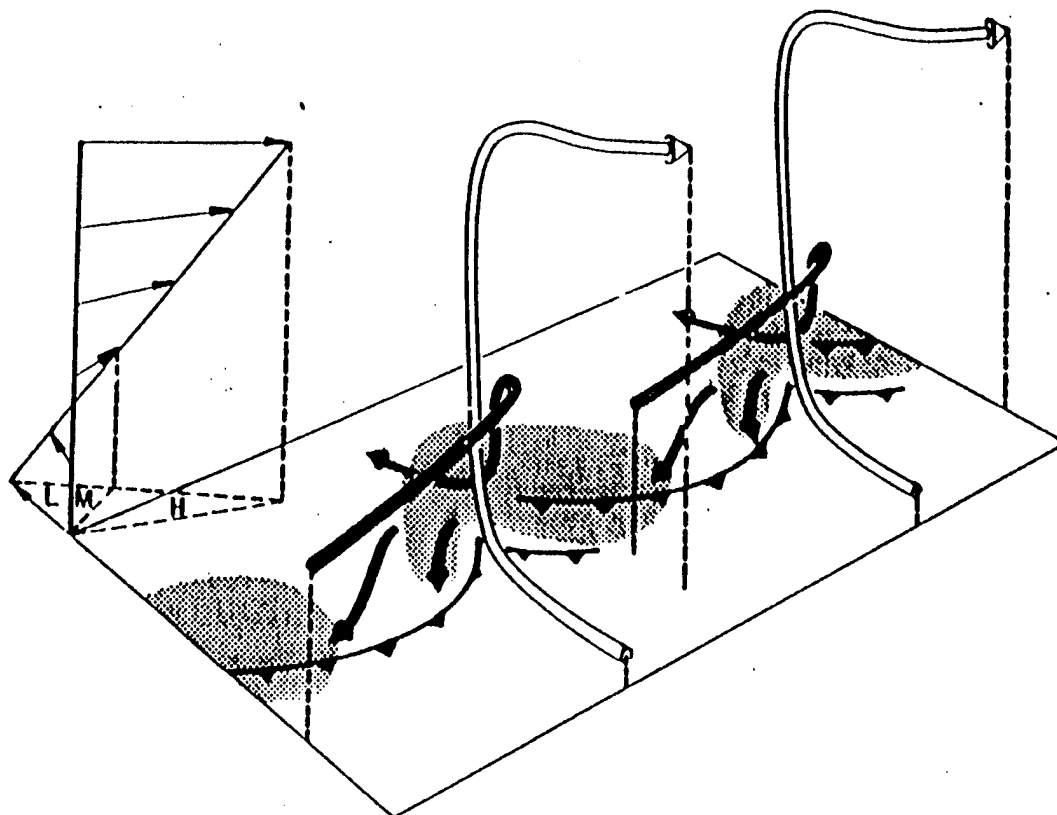


Fig. 3.2. Depiction of a supercell squall line propagating at an angle to the mean shear. Shear profile at left. Relative winds at low, middle and high levels indicated by L, M, and H respectively. Shaded area represents precipitation. Outflow boundary represented by cold front symbol. (Adapted from Rotunno et al., 1988)

#### **IV. UPPER-LEVEL JET STREAKS AND VERTICAL CIRCULATIONS**

##### **A. JET STREAKS**

Jet streams are narrow cores of high speed air embedded in much broader swaths of lower speed air. A jet streak is a local maximum of wind speed in the jet core. Jet streaks normally form when vigorous short waves propagate through a long wave trough or when weaker short waves come into phase with ridges to the south.

The necessity that the geostrophic wind field remain nearly non-divergent requires the entrance and exit regions of a jet streak to be convergent and divergent, respectively. This pattern will contribute to vertical motion which will be discussed in the next section. Jet streaks also produce the vertical wind shear required for sustained convection.

##### **B. JET STREAK INDUCED VERTICAL CIRCULATIONS**

Severe weather outbreaks, such as mesoscale convective systems and heavy snowfalls, have often been related to the position and intensity of upper-level wind maxima, i.e. jet streaks. Bluestein and Thomas (1984) state that much of the physical evidence involved in such a relationship depends upon the existence of a transverse vertical circulation.

Transverse vertical circulations are explained in terms of the ageostrophic component of the wind field. Ageostrophic wind speed ( $V_a$ ) is proportional to the horizontal accelerations experienced by an air parcel according to:

$$V_a = \frac{1}{f} \bar{k} \times \frac{D\bar{V}}{Dt}$$

which is obtained from the frictionless equation of motion. If the jet streak wind flow is zonal, the divergence is due to the divergence of  $\bar{v}$ , only: there will be divergence at the

left exit and right entrance and convergence at the left entrance and right exit Fig. 4.1 (Bluestein and Thomas, 1984). It can be seen in this figure that the convergence/divergence couplets are a result of the ageostrophic wind accelerations. The geostrophic wind divergence is usually negligible and is not considered. In the case where the jet streak is relatively close to the tropopause, static stability of the upper-atmosphere prevents vertical motion above the jet. Hence, below the divergent and convergent areas, strong vertical circulations may develop.

According to Bluestein and Thomas (1984), the rising branches of the vertical circulations may affect a statically stable environment in the following way:

- 1) decrease the static stability below the level of non-divergence;
- 2) cool the unsaturated layer to saturation releasing convective instability;
- 3) contribute toward moisture convergence at low levels and maintain a moisture supply to cumulonimbus towers.

The combined effect of both branches of a transverse vertical circulation may contribute to increasing the degree of convective instability in the exit region due to increasing low-level moisture and decreasing upper-level moisture by advection.

Positive vorticity advection is another mechanism that involves vertical motion in a jet streak. Considering a straight jet streak as in Fig. 4.1, the isotach pattern would result in shear induced vorticity, with cyclonic to the north and anticyclonic to the south. Given that the wind flow through the jet is faster than propagation speed, there would be PVA to the left of the exit and to the right of the entrance. Conversely, there would be NVA in the right exit and left entrance. Another way to look at this would be a frame of reference following a parcel (Bluestein, 1986). A parcel

exiting the jet through the left side would experience decreasing vorticity as it moves away from the region of shear induced, high cyclonic vorticity. This parcel must then experience divergence according to:

$$\frac{D(\zeta + f)}{Dt} = -\delta(\zeta + f) .$$

The pattern of divergence following a parcel is indicated in Fig. 4.2. It is evident from this figure that the pattern of divergence produced by vorticity advection enhances the transverse vertical circulation described earlier.

Curvature effects also contribute to the divergence/convergence couplets described above by increasing the vorticity and PVA/NVA . Relative vorticity defined as:

$$\zeta_r = \frac{V}{R} - \frac{\partial V}{\partial n} ,$$

is a combination of shear and curvature effects. The strongest cyclonic vorticity due to curvature is ahead of the wave axis, thereby contributing to strong shear vorticity at the left exit. This additive effect creates strong divergence at the left exit and results in strong ascent when combined with the transverse vertical circulation.

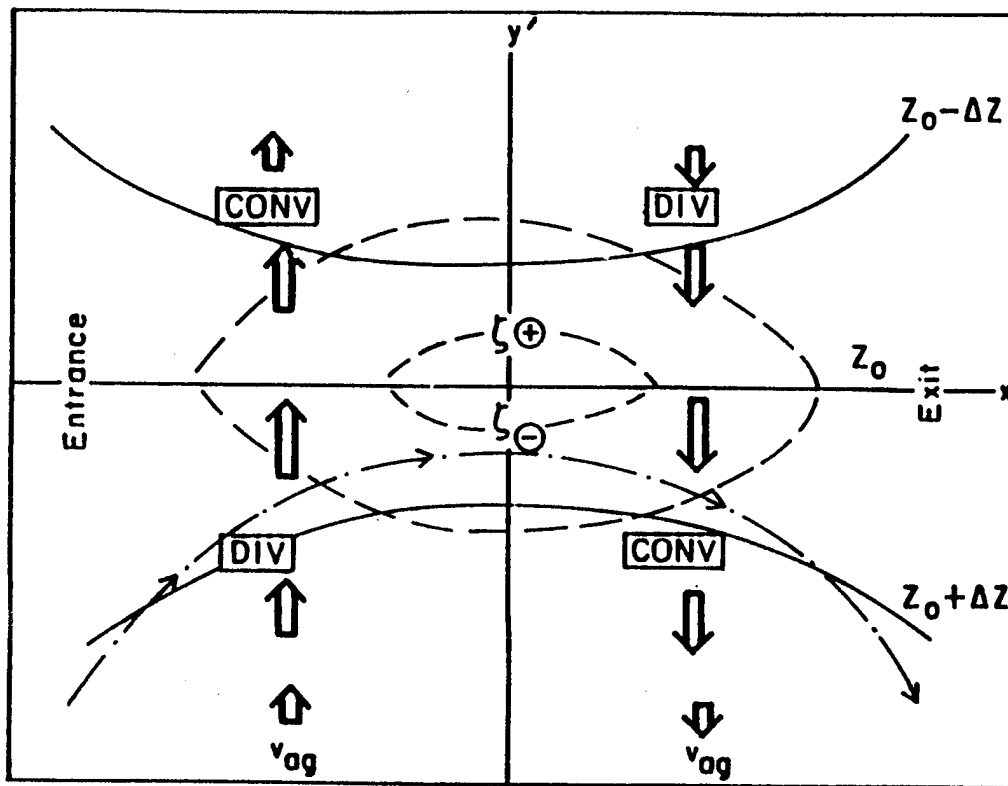


Fig. 4.1. Four quadrant model of jet streak. Isotachs are dashed lines. Dash-dot lines with arrow heads are parcel trajectories. Full curved lines are geopotential height contours. Double arrows indicate direction and magnitude of v-component of ageostrophic wind. (Adapted from Carlson, 1991.)

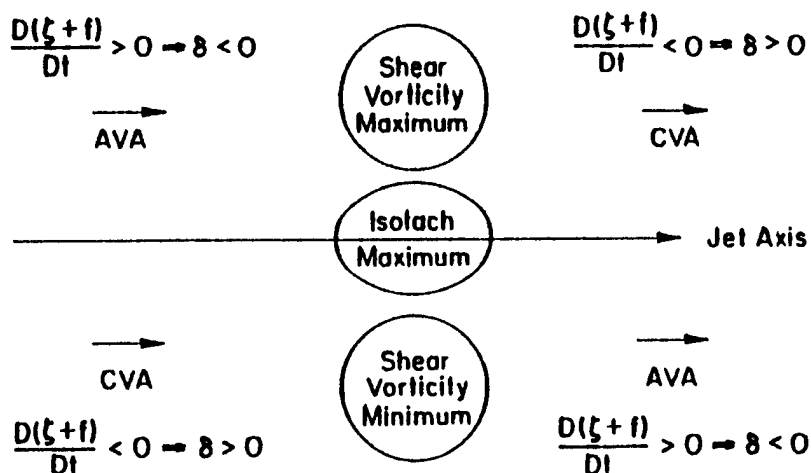


Fig. 4.2. Relation between vorticity changes experienced by an air parcel moving through a jet streak and the implied divergence.

## **V. INITIALIZATION DATA/MODEL DESCRIPTION**

### **A. ANALYSIS FIELDS**

#### **1. National Meteorological Center Gridded Analysis Fields**

Three-dimensional gridded analysis fields from NMC were used for the bulk of the evaluation of the pre-convection environment. These fields were plotted on a 45 by 30 degree grid over a United States background. This type of data facilitated the use of the *Visual* display software (see section V.B.).

These fields were comprised of the routine NMC synoptic data supplemented by an unusually high number of rawindsonde reports. Rawindsonde stations in the STORMFEST area provided more than 5,000 reports during the six weeks of the experiment.

#### **2. National Center for Atmospheric Research (NCAR) Enhanced Data**

##### **a. Composite Surface Data**

The NCAR collected data from a variety of sources during STORMFEST. This allowed the input of data of very high spatial and temporal resolution into various models. There were periods when data were collected at one-minute intervals. Five-minute intervals were routine for some stations. Most of the observational data from these stations went into NCAR's **composite surface data** set. This data set was composed of routine surface data such as air temperature, dew point, wind speed and direction, barometric pressure, altimeter, visibility, sky condition and precipitation. The composite data set consisted of hourly and five-minute averages of data. Most data were collected by the STORMFEST Data Collection Management Center (Cunning and Williams, 1993).

##### **b. Data Networks**

The STORMFEST Data Collection Management Center (SDCMC) collected data from many sources to attain as high a temporal and spatial resolution as possible. Data were

collected from NWS, Federal Aviation Administration (FAA), Department of Defense (DOD) and state agencies (Cunning and Williams, 1993). Additionally, NCAR installed 45 Portable Automated Mesonet (PAM) stations in the experiment domain, in Kansas, Missouri and Illinois, to supplement the existing stations. The combination of these networks of reporting stations provided very high resolution analysis data.

## **B. ANALYSIS SOFTWARE**

### **1. Visual**

*Visual* is a data display program. *Visual* displays gridded data and diagnostic fields computed from the gridded data. It was written by Wendell Nuss from similar coding developed at NCAR and uses NCAR Graphics utility routines. *Visual* was used for most of the pre-convection environment analysis. The coarse gridded Global Data Assimilation (GDAS) Final Analysis fields were interpolated to the 35 km *Visual* grid for display and manipulation.

*Visual* allows the data to be manipulated and plotted in various ways as well as plotting vertical cross-sections and display of GOES satellite imagery. For this analysis *Visual* was used to display various horizontal fields, as well as plotting vertical circulation cross-sections to determine vertical motion. *Visual* also was used to plot NCAR mesonet and composite surface data for mesoanalysis.

### **2. NCAR Zeb Software**

NCAR has developed a CD-ROM set with all of the STORMFEST observational data, including satellite imagery, surface radar reflectivity and doppler data and wind profiler data. *Zeb* is an interactive display package that has been included with the CD-ROM set. *Zeb* is a comprehensive program that provides a variety of displays including surface plots, vertical cross-sections, Skew-T and profiler time-height plots. It is a windows-based program designed to work on a Sun workstation.

The Zeb software was used to analyze the radar reflectivity data, Skew-T data and wind profiler plots. User manipulation of the profiler data was instrumental in evaluation of the strength of jet streak over the MCS genesis region.



## VI. PRE-CONVECTION ENVIRONMENT

### A. SYNOPTIC FORCING

#### 1. Overview

A very complex surface low pressure associated with a broad upper-level trough was situated over the southwestern U.S. on 08 March 1992. The evolution of these features can be followed in the surface and 500 mb level analyses for 1200Z 08 March, 0000Z and 1200Z 09 March (Figs. 6.1 through 6.3). The contoured data are *Visual* analyses of the NMC GDAS fields. The surface feature symbols are taken from the NMC U.S. surface hand analyses valid at the same times. The main surface feature at 1200Z 08 March 1992 was a deepening 1002 mb low pressure center over Colorado (Fig. 6.1.a) with a cold front trailing south across New Mexico into northern Mexico. In the middle and upper-troposphere a deep low height center was positioned in the trough over southeast California (Fig. 6.1.b). This low height center moved rapidly to Colorado maintaining its intensity over the next twelve hours (Fig. 6.2.b). A vigorous short wave associated with this low moved northeast to the Texas panhandle digging southeast to central Texas by 0000Z 09 March 1992. This produced strong southwest mid-tropospheric flow over Texas and Oklahoma by 0000Z. The surface low pressure center deepened to 994 mb and moved to the west Kansas border at this time (Fig. 6.2.a) with its trailing cold front extending from the low south across the Texas panhandle then south-southwest to the Big Bend area. A dryline 150 miles in advance of the front at 1200Z was analyzed by NMC to be 100 miles in advance of the front at 0000Z extending from southwest Kansas south to Big Bend. Severe convective cells were developing along the dryline by 0000Z. The numerous cells quickly evolved into a severe squall line. This is quite evident in Fig. 6.4, a composite of NWS weather radar reflectivity data overlaid on a GOES enhanced

infrared image, both valid at 0300Z 09 March 1992. Through the next twelve hours, the surface low propagated into central Kansas, filling to 999 mb (Fig. 6.3.a). The cold front, as analyzed by NMC, extended from the low at that time southwest to the Texas panhandle then northwest across the Rockies into Idaho and Montana. The upper-level low and short wave moved rapidly northeast through this period as the low deepened (Fig. 6.3.b). A significant 200 mb jet streak with maximum winds of 140 knots developed in central Texas by 0000Z on 09 March (Fig. 6.5.a). The left exit was located just north of Dallas. This feature moved slightly east and maintained intensity through the next twelve hours (Fig. 6.5.b). These synoptic-scale features interacting with the dryline and the sloping topography forced the severe convection and its evolution, thereby producing a long-lasting squall line.

The pre-convection environment has been studied vigorously with coarse gridded fields, satellite imagery, radar reflectivity data and wind profiler data. The satellite imagery and gridded fields indicate that the severe convection was associated with a complex interaction of synoptic and mesoscale forcing mechanisms. A very vigorous upper-level jet streak played a significant role in determining the severity of the convection. Synoptic-scale lifting associated with low-level convergence of warm, moist air east of a strong dryline also contributed. Advection of warm, dry air in the mid-troposphere, originating from the elevated plateaus of Mexico, enhanced the instability of the atmosphere. All of this created an environment waiting for a "kicker" to release the instability and initiate deep convection.

The lifting required to initiate the convection was available from a variety of sources. Synoptic-scale sources were: 1) the upper-level jet streak, which provided lifting at the left exit region due to positive vorticity advection and divergence of the ageostrophic wind creating a transverse

vertical circulation, and 2) the propagation of a cold front into western Texas, which also contributed to vertical motion. A mesoscale initiation mechanism may have been **underrunning**. Schaefer (1986) has indicated that ageostrophic circulations associated with upper-level disturbances often advect the unstable surface-layer air to the northwest. Once the air flows out from under the capping inversion, especially violent convection occurs.

## **2. Atmospheric Stability Analysis**

Low-level gridded data indicates strong moisture convergence and warm advection over central and eastern Texas. A contoured analysis of potential temperature at 1000 mb for 1200Z 08 March 1992 and 0000Z 09 March 1992, Fig. 6.6, and a contoured mixing ratio analysis for the same times (Fig. 6.7), clearly show an intrusion of warm and moist air into central Texas and across the Texas and Oklahoma panhandles. This allowed the development of a deep, moist layer near the surface. Gridded GDAS wind fields and profiler data indicate that in the mid-troposphere, from 800 to 600 mb, much drier and warmer air was advected over the genesis region, a **Mexican plume**, as described by Schaefer (1986). This pattern caused the evolution of a deep layer of potentially unstable air. Fig. 6.8 is a sequence of soundings from Norman, Oklahoma on 08 and 09 March 1992. The near-surface layer moistened from 2000Z 08 March 1992, (a), through 0200Z 09 March 1992, (c), as a strong inversion developed in the 850 to 800 mb layer. GDAS mixing ratio and wind data reveal that the inversion evolves in response to dry, warm advection from the southwest. The mid-troposphere cools and dries during this period with the lapse rate being nearly dry adiabatic at 0200Z 09 March 1992. After 0200Z, the sounding became convectively mixed with the passage of the squall line, (d), and began to dry out by (e), 0800Z 09 March 1992.

The sounding at 0200Z clearly indicates deep, potential

instability. Once a parcel burst through the inversion, it was positively buoyant up to the tropopause and was likely to overshoot. Overshooting tops are evident in the three large cells over southwest Oklahoma and just south in Texas in Fig. 6.9.

### **3. Surface and Lower-Tropospheric Discussion**

Figs. 6.1 - 6.3 depict a very complex situation over the Southwest. A frontal system extending from Utah southeast into Colorado then south across eastern New Mexico into Mexico moved rapidly east with a weak low over northeast New Mexico deepening as it moved northeast. A significant dryline is indicated extending south along the eastern panhandle of Texas then southwest into the Big Bend area. Careful inspection of the STORMFEST enhanced data however, might suggest placing the dryline 60 miles further west as indicated in Figs. 6.10 and 6.11. Figs. 6.10 and 6.11 are hand analyses of the sea level pressure and dew point temperatures of the enhanced data at 1800Z and 2100Z, 08 March 1992. Dew point temperature differences across this dryline were as high as 35 to 40 °F.

A considerable moisture gradient along the dryline is also evident at this time. The vectors in Fig. 6.7, representing the 1000 mb wind field, depict convergence of mass and momentum along the dryline boundary, undoubtedly resulting in the formation of the low-level jet. The low-level jet, although not resolvable in the gridded data analysis, is identifiable in profiler data. Low-level or nocturnal jets typically evolve due to differential heating of the higher mountain slopes of the Rockies. Increased insolation of the upper slopes creates a pressure gradient force. A coriolis response generally causes the induced jet to flow from the south. Fig. 6.12 is a series of profiler observations from Purcell, Oklahoma (30 miles south of Oklahoma City) for 0 to 4000 meters. The observations in the 1400 to 2400 meter layer

are 40 to 50 knots (recorded in m/s). This observation, and others not shown, verify the existence of the low-level jet. This inevitably enhances the lifting along the boundary due to increased warm air advection.

Moisture pooling in eastern Texas, ahead of the dryline, is apparent in Fig. 6.7.b, 0000Z 09 March 1992, at 1000 mb; moisture pooling is even stronger at 850 mb (not shown). Moisture pooling into the genesis region was aided by the low-level jet.

#### **4. Upper-Level Jet Streak Analysis**

The presence of a very vigorous upper-level jet streak may be the key to the severity of this mesoscale convective system. The jet streak enhances vertical motion in two ways: 1) divergence associated with positive vorticity advection in the right entrance and left exit regions, and 2) divergence associated with the ageostrophic wind accelerations/decelerations also in the right entrance and left exit regions. Dines compensation correlates upper-level divergence/convergence with underlying convergence/divergence, and upward/downward motion between the levels involved. This contribution to vertical motion, combined with frontal and dryline lifting, resulted in the most spectacular convection.

Fig. 6.13, a gridded 200 mb wind field isotach analysis for 0000Z 09 March 1992, exhibits a 140 knot jet speed maximum over central Texas with the left exit over the genesis region. The strength of this particular jet streak results in sustained, severe convection through two mechanisms: 1) the aforementioned vertical motion, and 2) strong vertical wind shear. The sheared cirrus clouds can readily be seen blowing off to the northeast in Fig. 6.9.

Fig. 6.14, a time series of wind profiler data for Purcell, Oklahoma (30 miles south of Oklahoma City), clearly

illustrates that the jet streak was actually much stronger than the gridded data indicates. The profiler recorded winds of 170 to 190 knots at 13400 meters from 0000Z to 0100Z 09 March 1992. These winds may be suspect when considering the direction of the surrounding data. This report does however, suggest that the jet streak was stronger than indicated in the gridded field, and likely further north than indicated. The profiler shows 50 knots of wind shear between 0 and 10000 meters and 100 to 110 knots of wind shear between 10000 and 13400 meters.

The strength of this jet streak resulted in strong positive vorticity advection (PVA) into the genesis region. Fig. 6.15, the contoured 200 mb relative vorticity analysis with wind vectors valid for 0000Z 09 March 1992, shows the strong PVA over the genesis region. Given that the actual jet streak was stronger than the gridded data suggests, it is logical to assume that the PVA was actually stronger than this figure suggests.

An analysis of upper-level divergence indicates that the jet streak was very strong also. Fig. 6.16, an analysis of 300 mb and 200 mb divergence for 0000Z 09 March 1992, indicates divergence at the left exit for the 300 mb level. The 200 mb analysis, however, suggests that the stronger divergence was located at the right entrance region. The 200 mb ageostrophic wind analysis, however, also suggests that the strongest divergence is at the right entrance. This confirms that the jet streak interacting with other processes results in such severe convection, and not the jet streak acting uniquely.

#### **5. Vertical Motion Discussion**

The analyzed synoptic data indicates that the convective system evolved in an environment of strong ascent and strong vertical wind shear. In previous sections, the ascent has been attributed to an interaction of synoptic-scale and mesoscale forcing mechanisms. Fig. 6.17.a, a cross-section of vertical

motion across the dryline at 0000Z 09 March 1992, indicates that forced ascent up the dryline boundary is a much more dominant contributor to vertical motion (location of cross-section indicated by line between X's in Fig. 6.12). This ascent is likely due to three factors: 1) forced ascent due to motion of the cold front, 2) PVA aloft associated with the jet streak, and 3) the transverse vertical circulation. It is likely that the ascent, although enhanced by the PVA aloft and dryline motion, is primarily due to the transverse vertical circulation associated with the left exit of the jet streak. This is strongly supported by Fig. 6.17.b, a cross section (extending from Albuquerque to St. Louis) of vertical motion resulting from the ageostrophic component of the wind only. The largest vectors are located in the vicinity of the dryline at the left exit of the upper-level jet streak at the extreme left side of the cross-section.

## **B. MESOSCALE FORCING**

Examination of the 1800Z 08 March 1992 and 0000Z 09 March 1992 NMC United States surface analyses reveals a very significant dry line feature (position indicated on Figs. 6.1 - 6.3). The dryline marks the boundary between the moist, warm Gulf of Mexico air being advected north into the Midwest, and the advection of much drier and cooler air down the slopes of the Rockies and into the Texas/Oklahoma panhandles. Dew point differences across this boundary range as high as 40 °F.

More accurate positioning of the dryline can be seen in Figs. 6.10 and 6.11. A significant detail to notice is that by 2100Z, the cold frontal trough propagates into the dryline. This coincides with the initiation of convection in the genesis region.

The cross-section (Fig. 6.17.a) across the Texas panhandle indicates that the lifting occurs right at the position of the dryline. This figure also indicates forced

subsidence west of the dryline over the slopes of the eastern Rockies. This contributes to warming and drying west of the dryline boundary. This is typical of the lee side trough and dryline according to Martin et al. (1995).

The dryline becomes quite evident in the infrared imagery of Fig. 6.18 and 6.19, as the convection develops and becomes severe. The second image, Fig. 6.19, indicates the dryness behind the dryline, with the warmer temperatures of the surface being recorded by the satellite radiometer. This results in the dark area behind the convective clouds on the image. Fig. 6.4 identifies the dryline very accurately. The dryness behind the line is evident by the darker brightness return in the infrared image. Cumulus and cumulonimbus form precisely on the line as indicated by the infrared imagery as well as the radar reflectivity data.

A thorough analysis of the large-scale and mesoscale data indicates that the extreme potential instability evolved in the lower and middle-atmosphere over the genesis region. This is due to moisture convergence ahead of the dryline enhanced by the low-level jet and dry, warm advection aloft from the southwest. This instability was then released in the form of severe convection. The releasing mechanisms were the propagating cold front and associated jet streak aloft. Fig. 6.20, an enhanced infrared GOES image with radar reflectivity and STORMFEST enhanced data set dew point analysis overlaid, indicates these mechanisms nicely. Cumulus associated with the front is located just ahead of the moisture gradient indicating the position of the dryline and front. (This corellates well with Fig. 6.11.) Convection is well developed in the moisture pool ahead of the front and dryline.

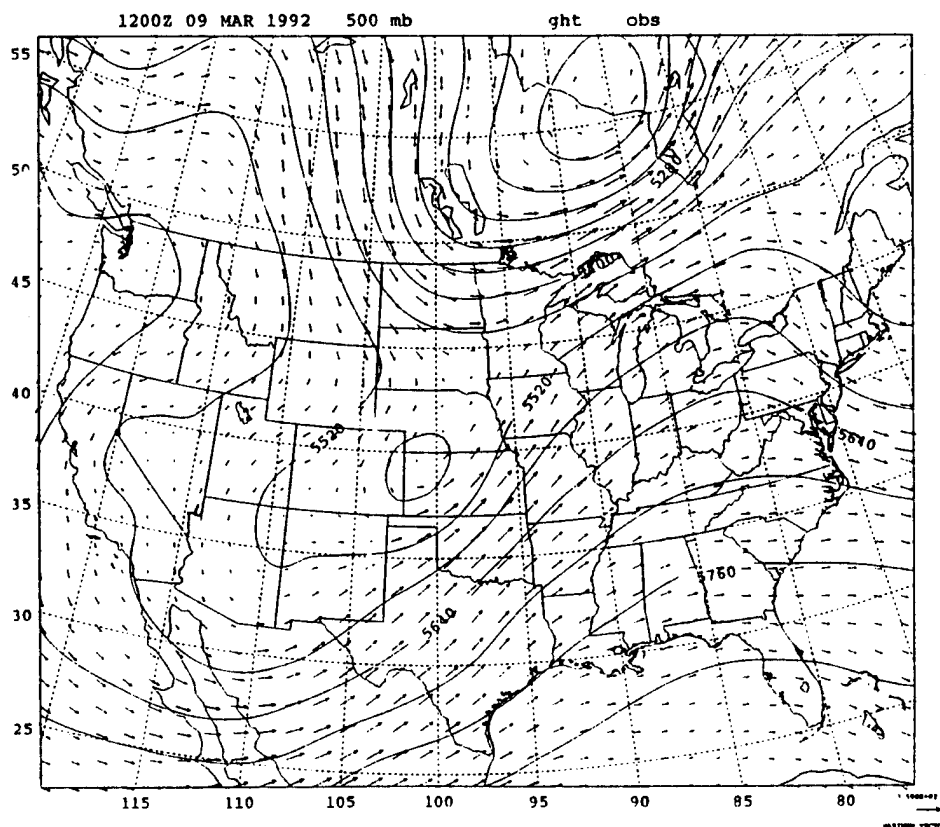
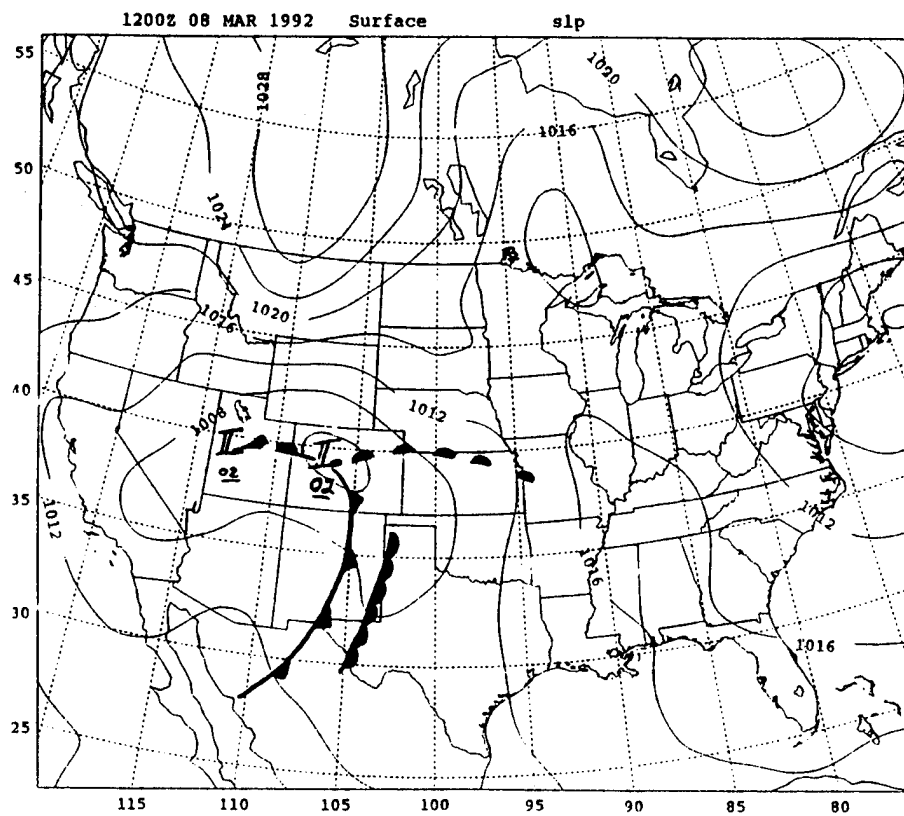


Fig. 6.1. Visual sea level pressure contoured analysis of NMC Final GDAS data with NMC U.S. hand analysis features drawn on from the same valid time (a), and Visual 500 mb geopotential height contour analysis (b) for 1200Z, 08 March 1992.

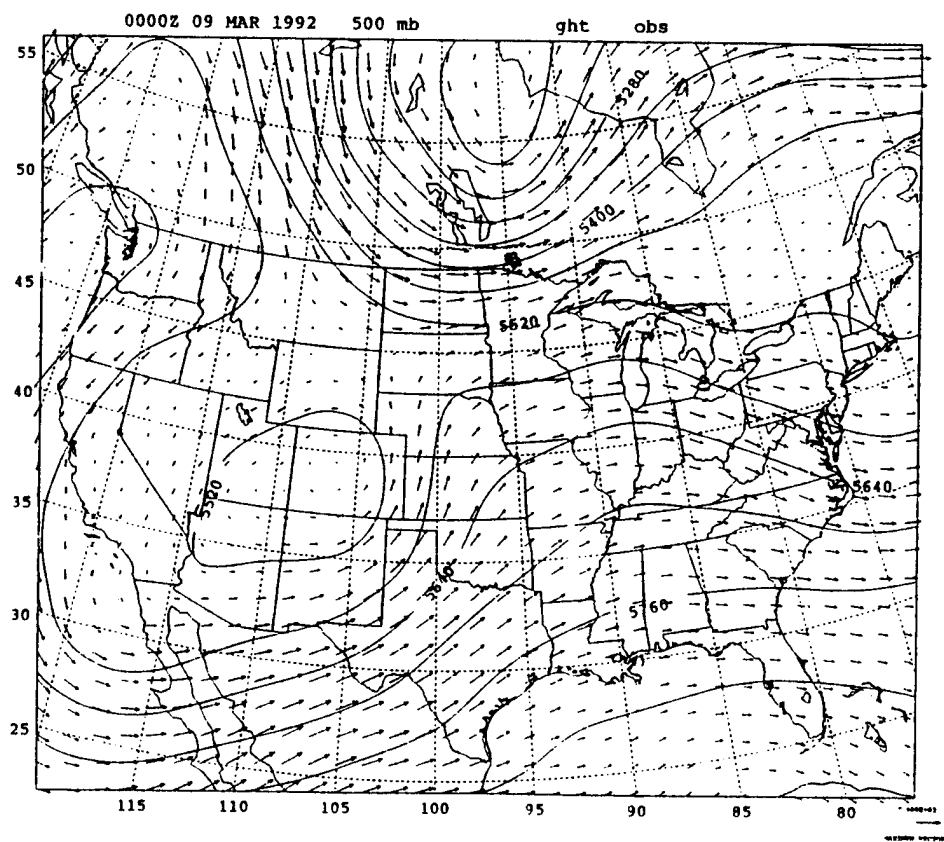
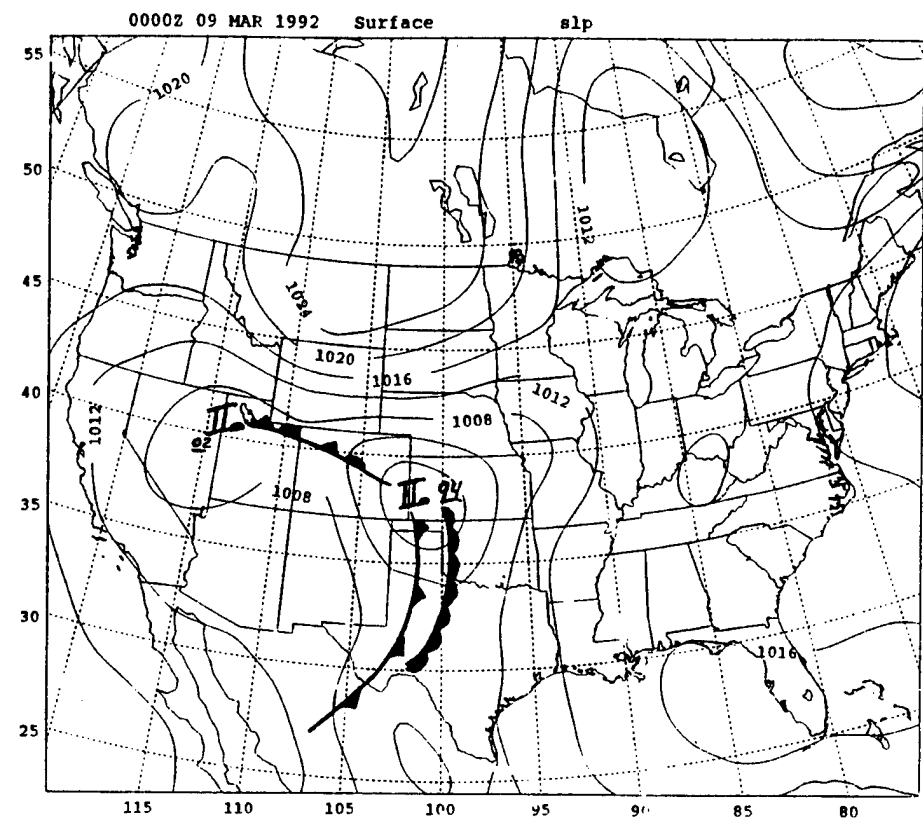


Fig. 6.2. Same as Fig. 6.1 except for 0000Z, 09 March 1992.

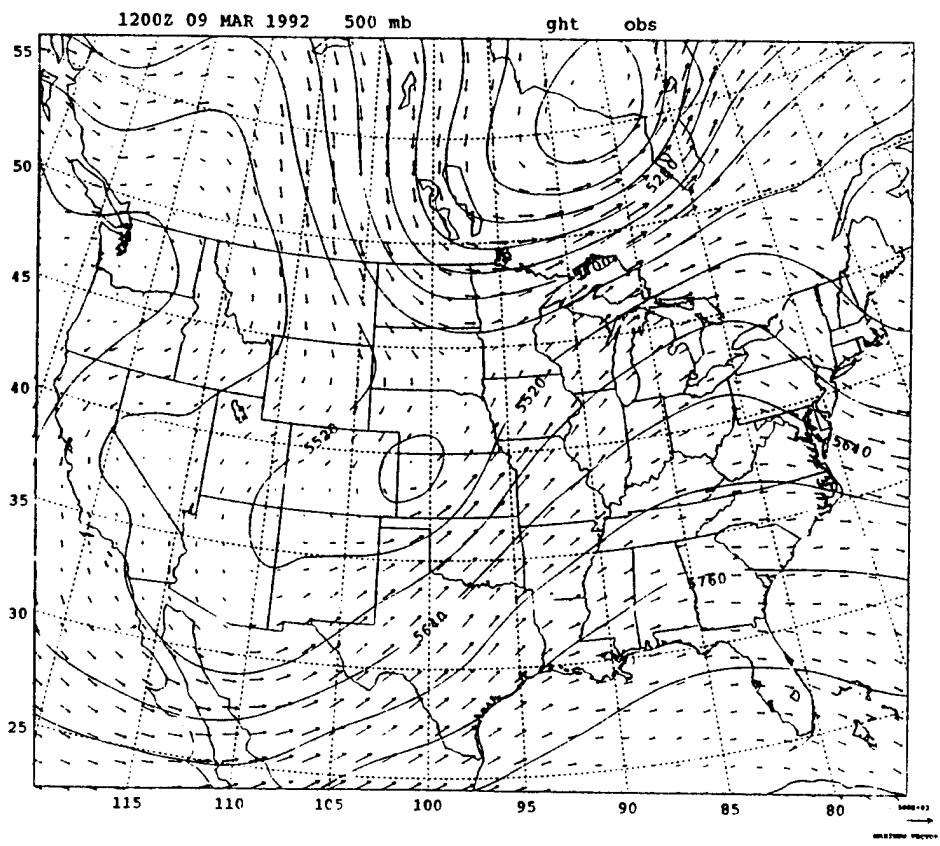
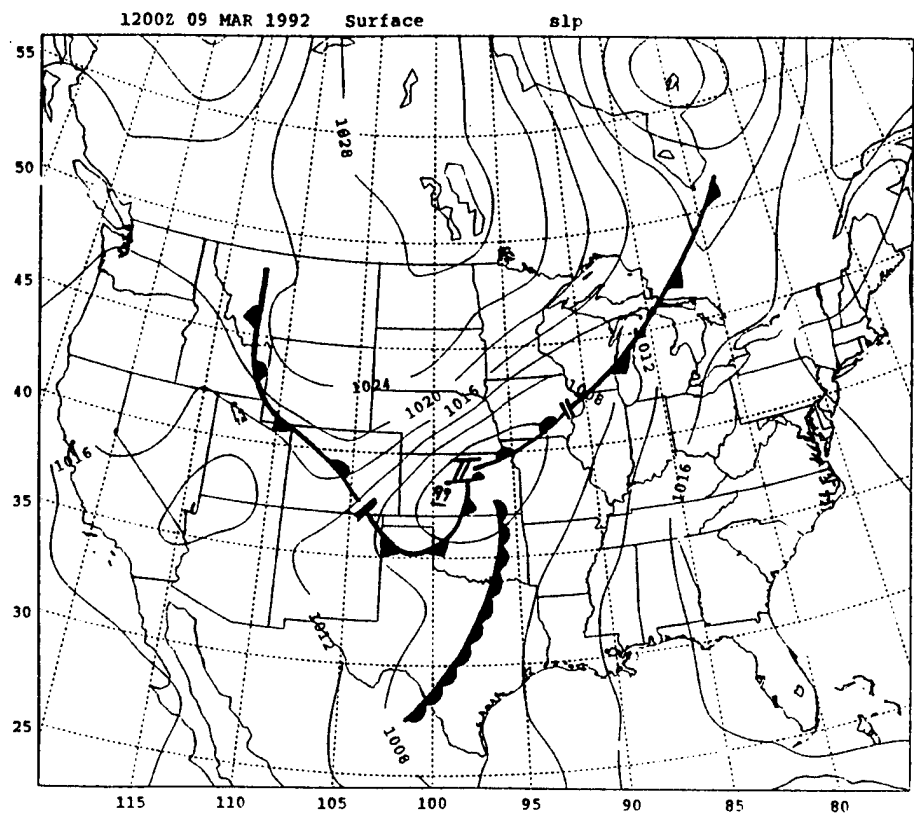


Fig. 6.3. Same as Fig. 6.1 except for 1200Z, 09 March 1992.

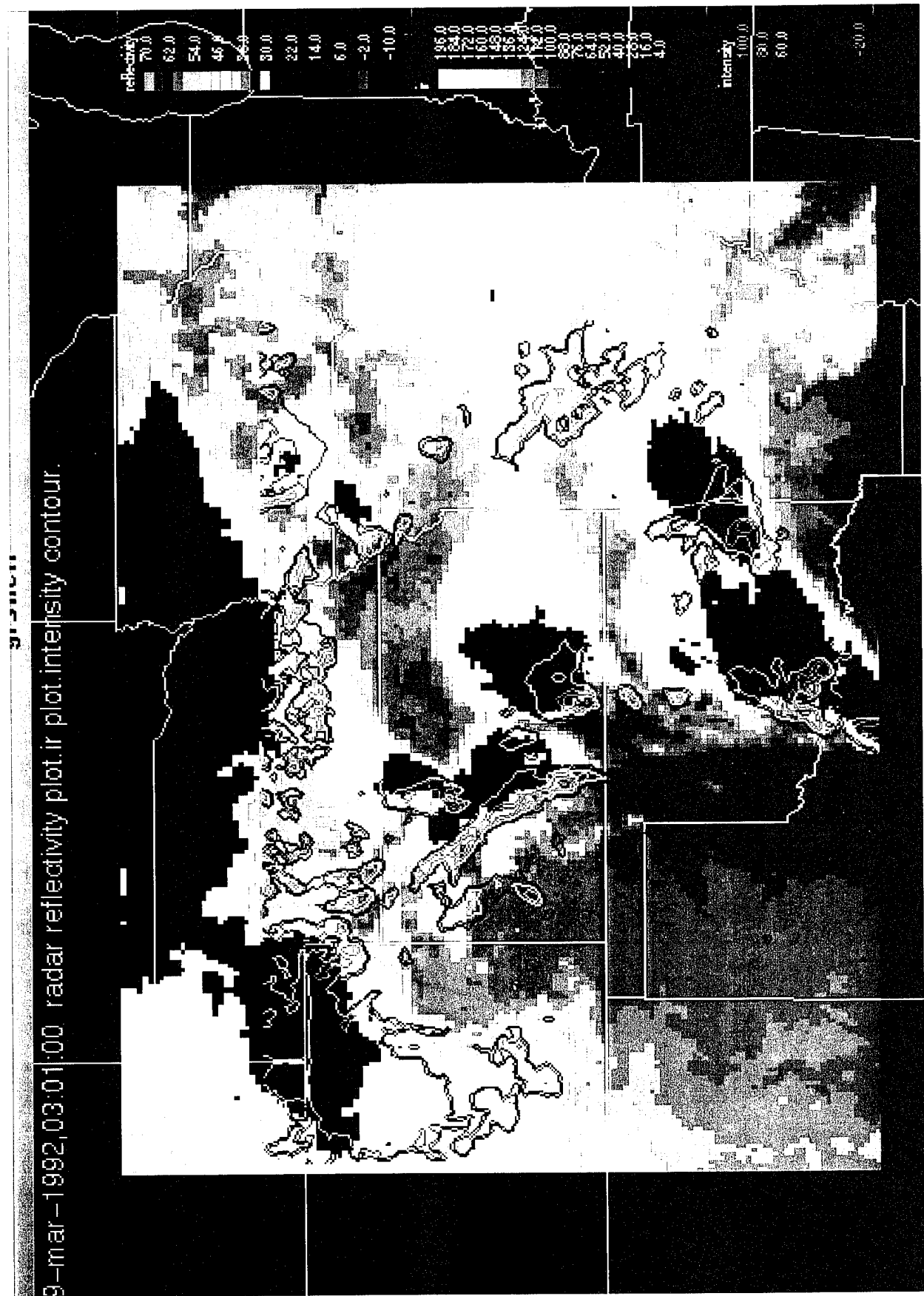


Fig. 6.4. 0301Z 09 March 1992 GOES enhanced infrared image with composited NWS weather radar reflectivity data overlaid.

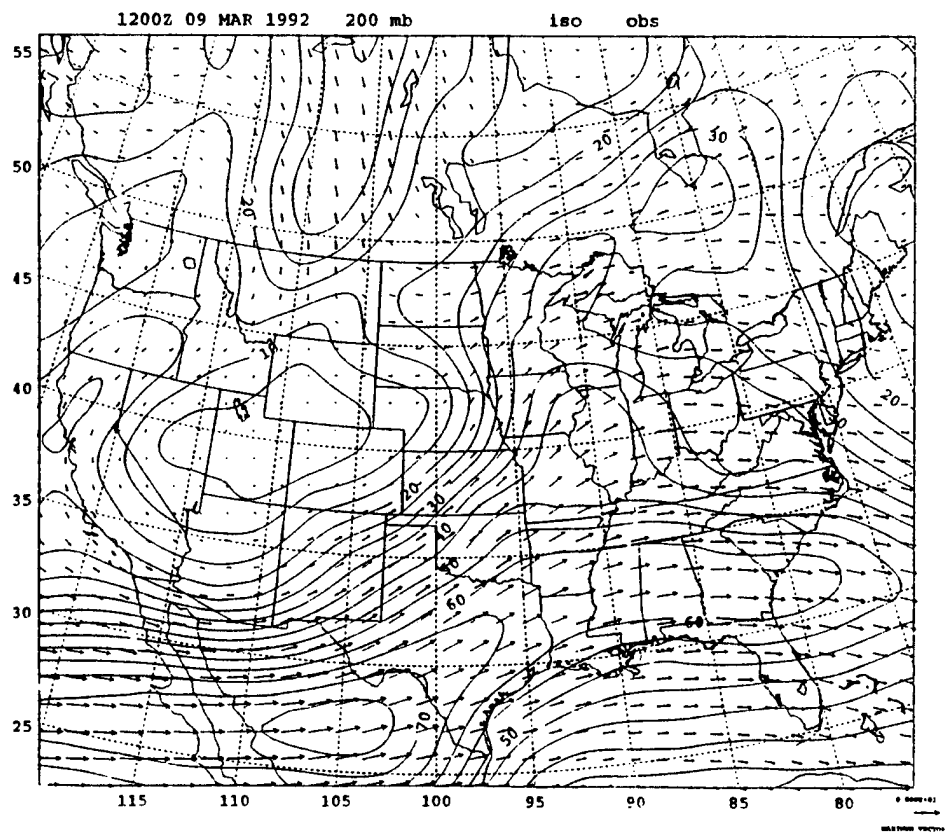
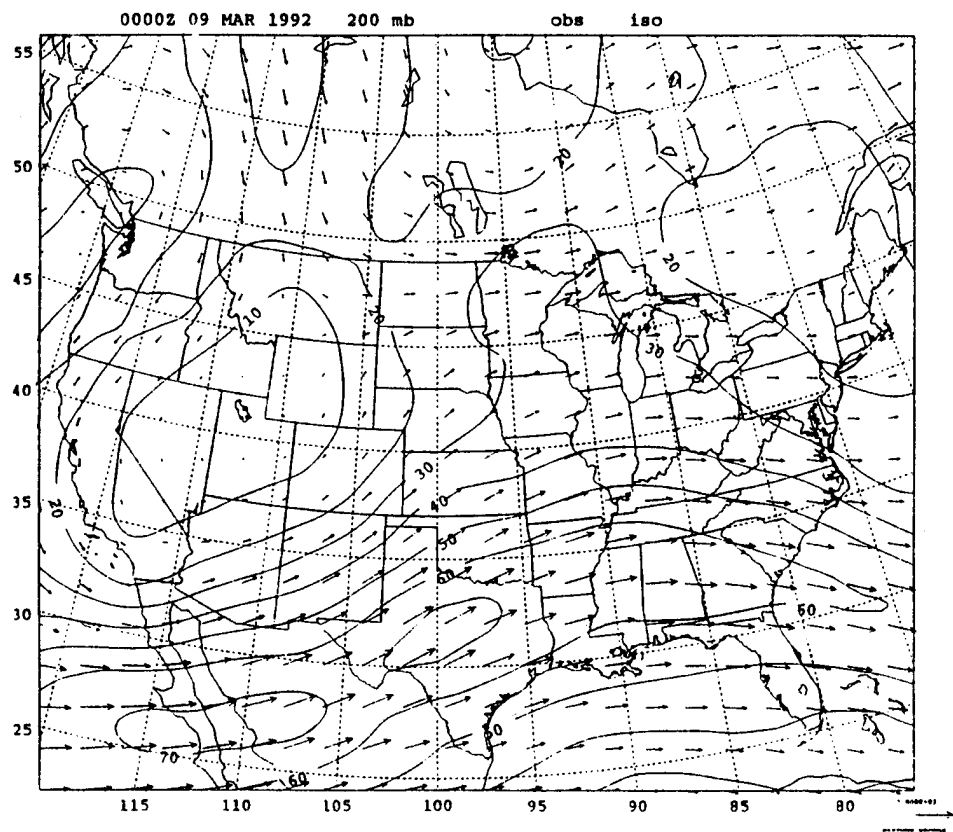


Fig. 6.5. Visual isotach analysis of NMC Final GDAS 200 mb data with wind vectors overlaid for 0000Z (a), and 1200Z (b) 09 March 1992.

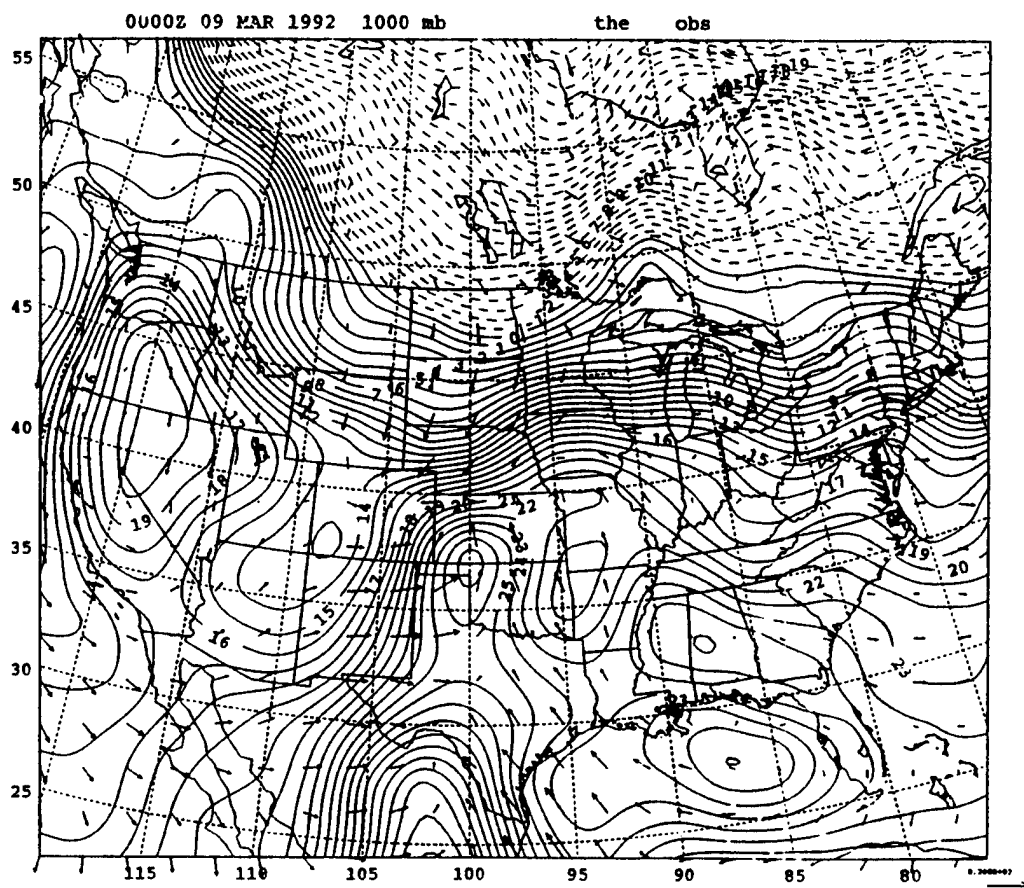
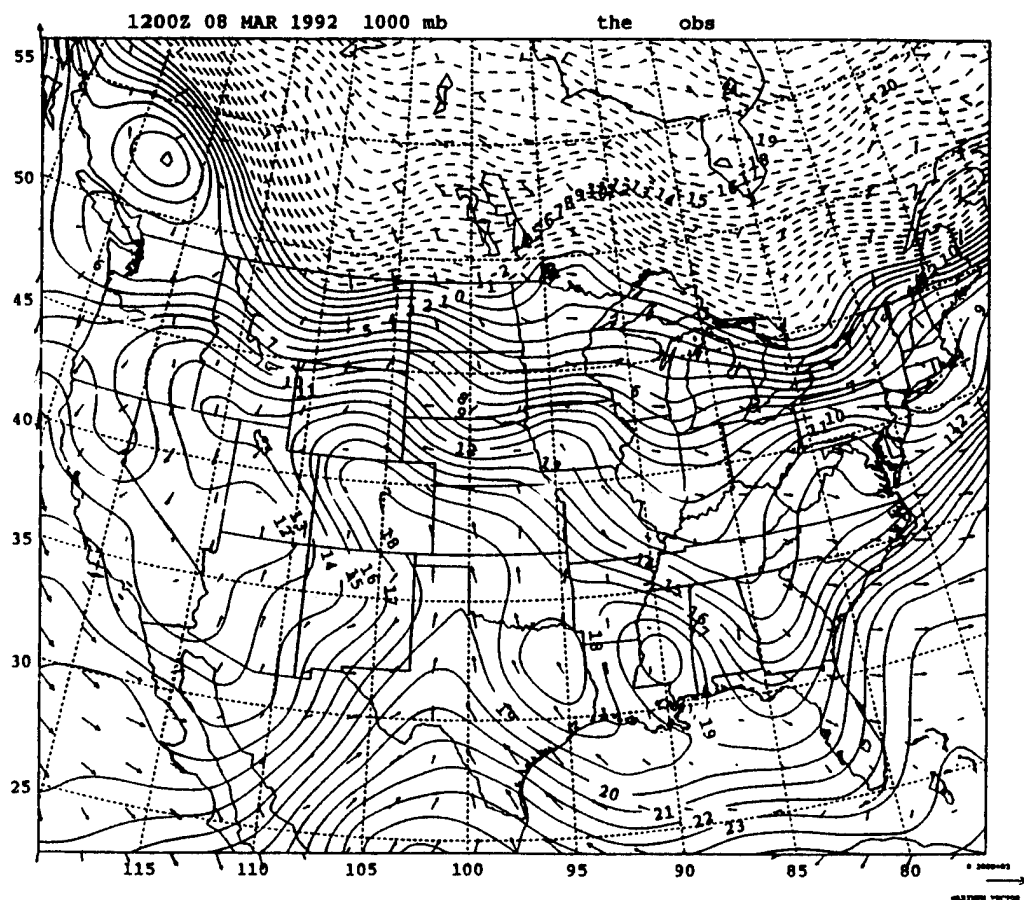


Fig. 6.6. Potential temperature with wind vectors at 1000 mb. Dashed contours are negative values.

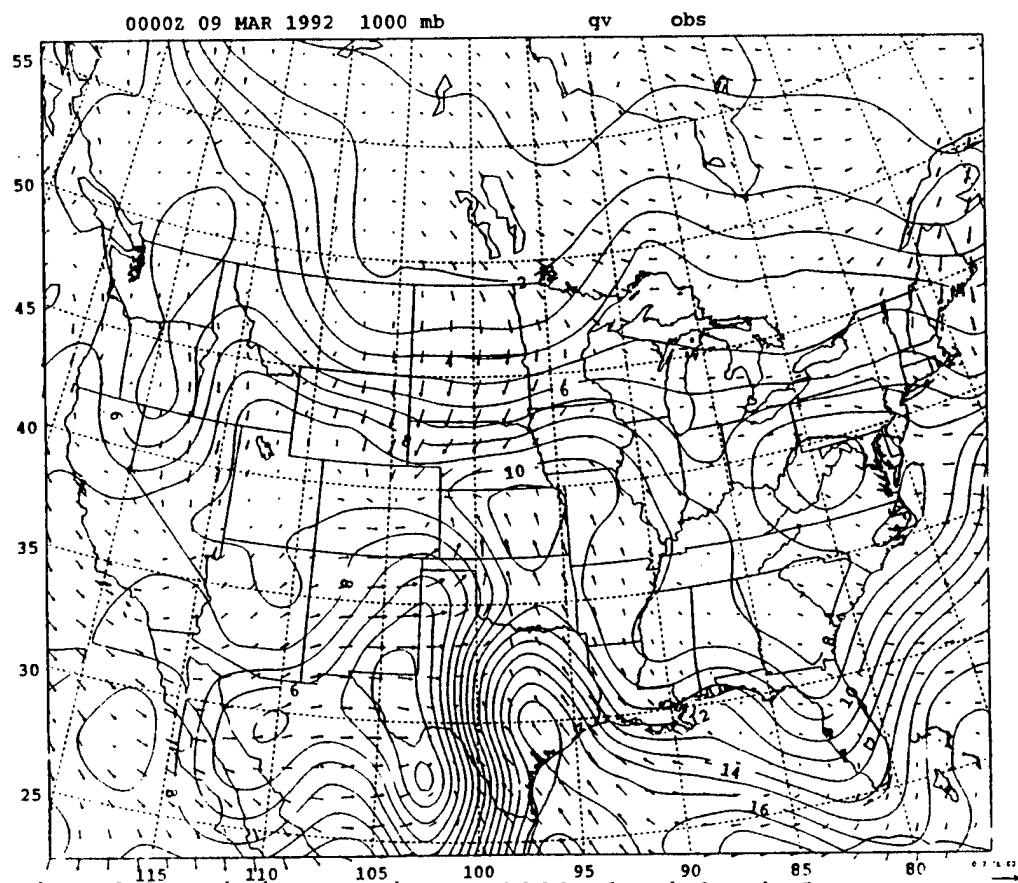
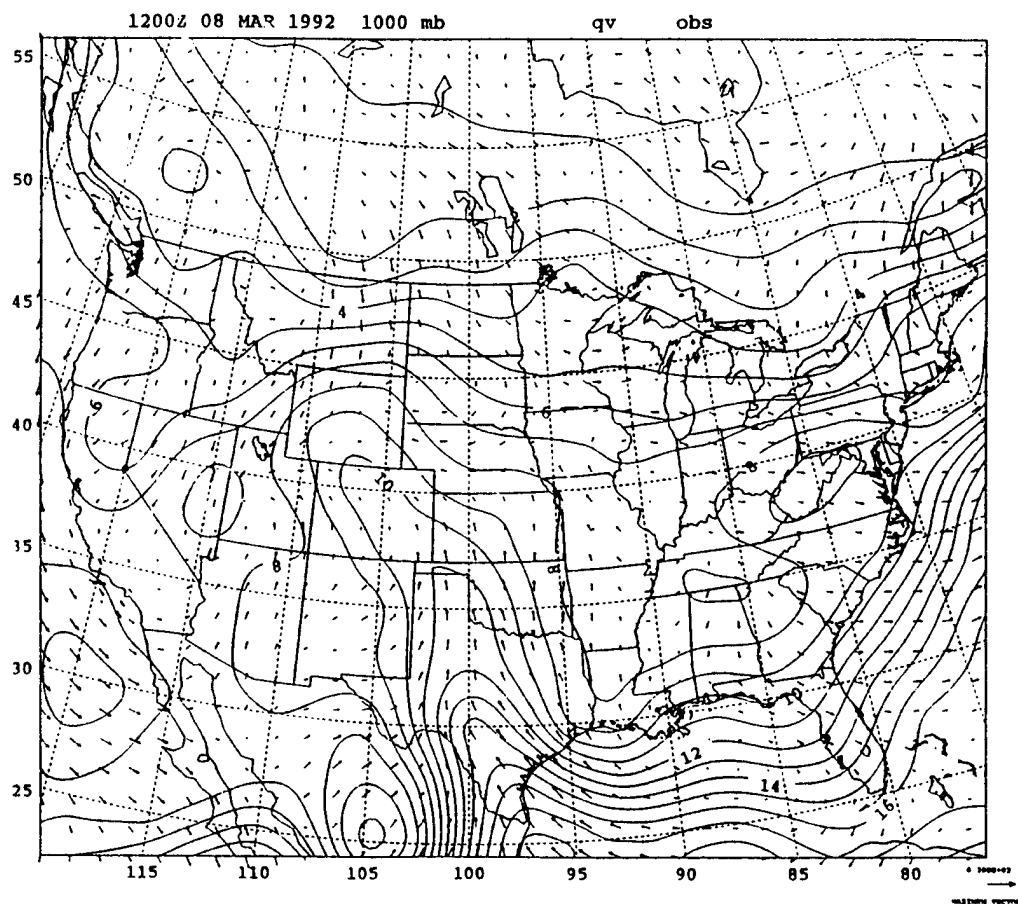


Fig. 6.7. Mixing ratio at 1000 mb with wind vectors overlaid.

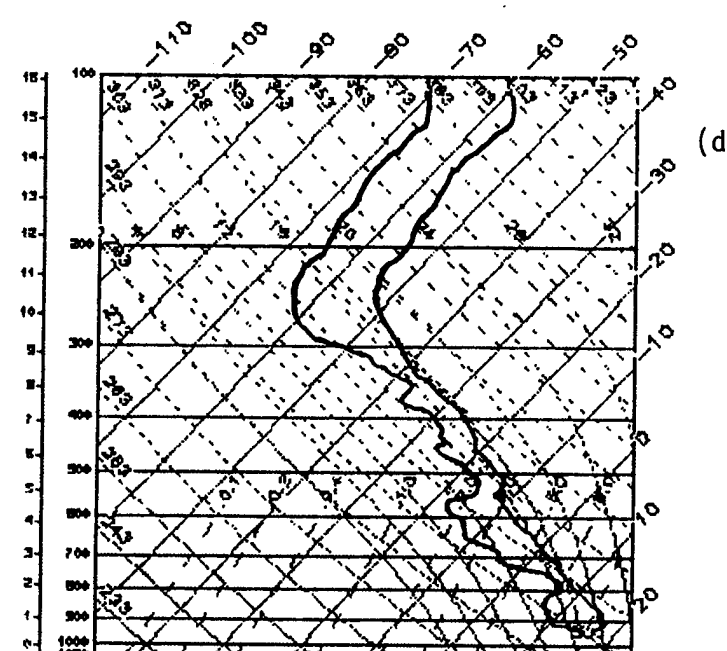
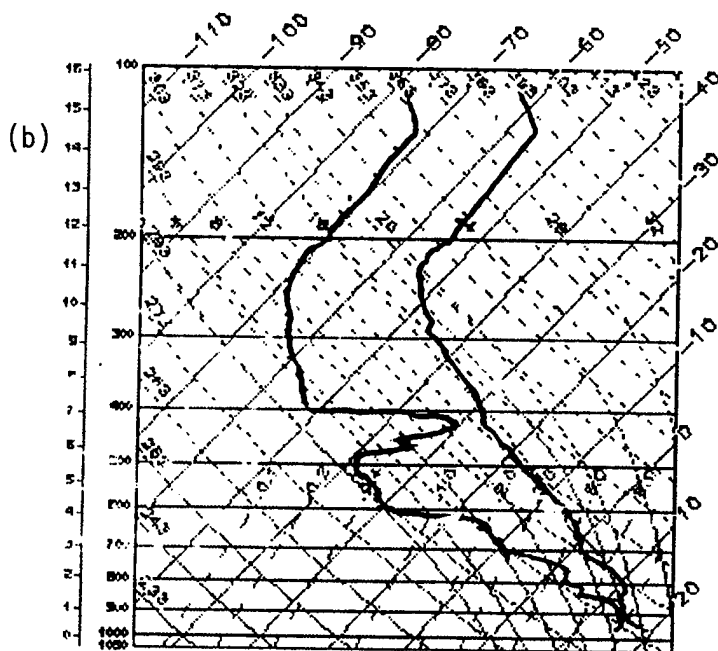
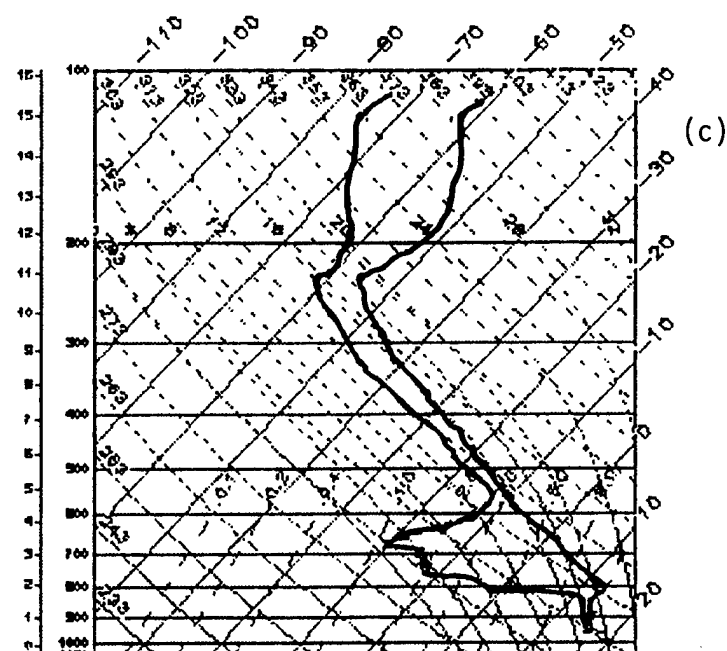
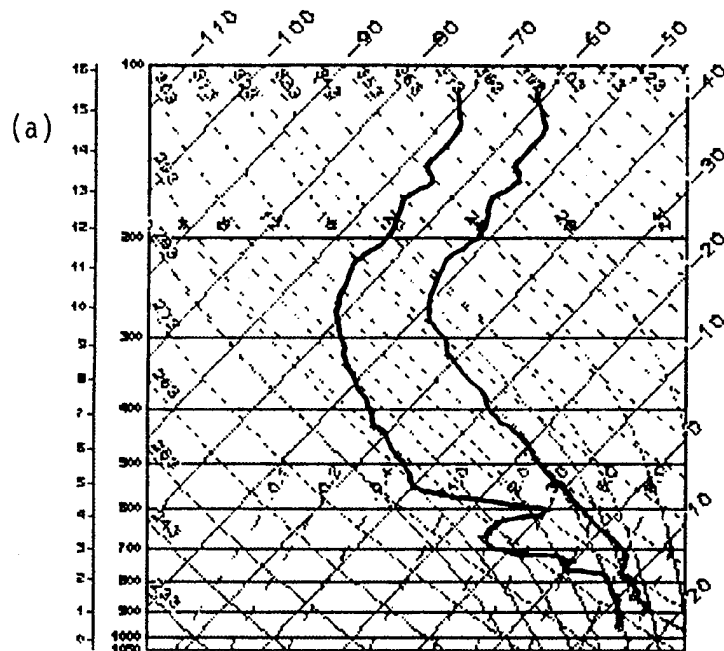
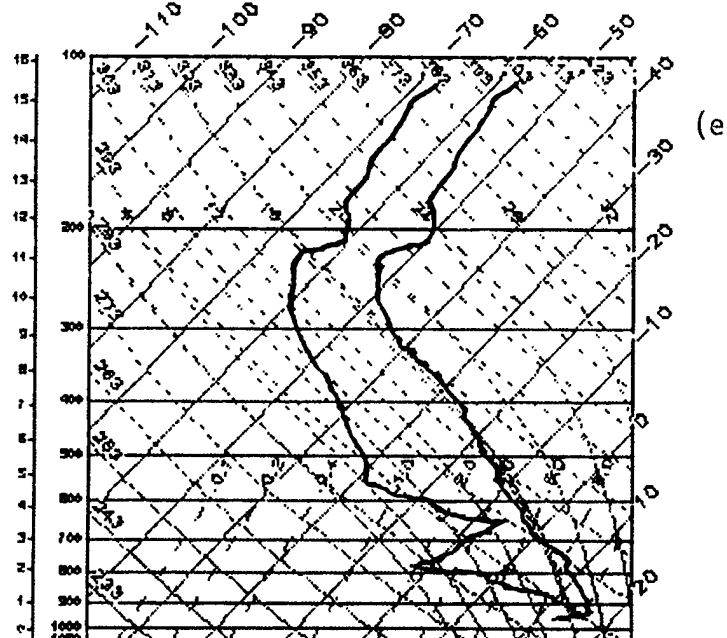


Fig. 6.8. Sequence of soundings from Norman, Ok.  
 (a) 20Z 8Mar92, (b) 00Z 09Mar92, (c) 02Z 09Mar92, (d) 05Z 09Mar92, and (e) 08Z 09Mar92.



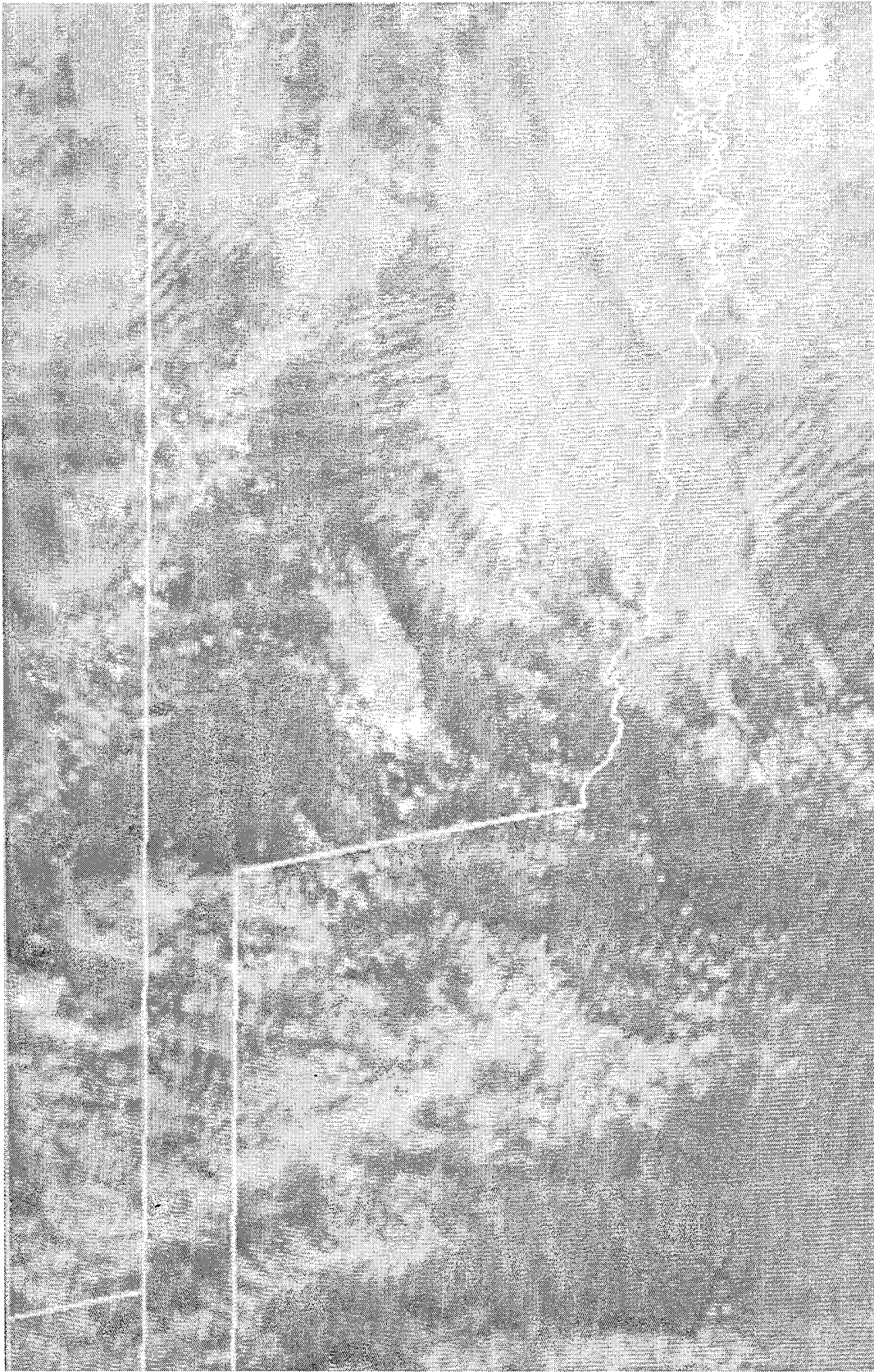


Fig. 6.9. 2300Z 09 March 1992 Visible GOES image.



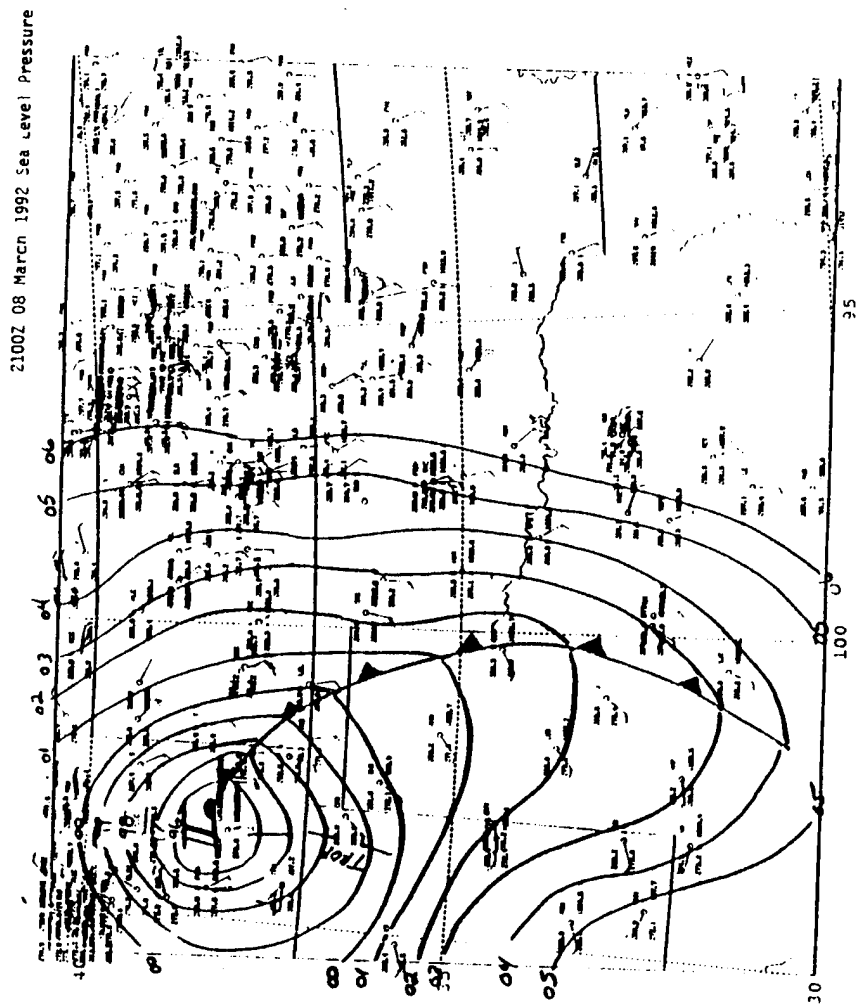
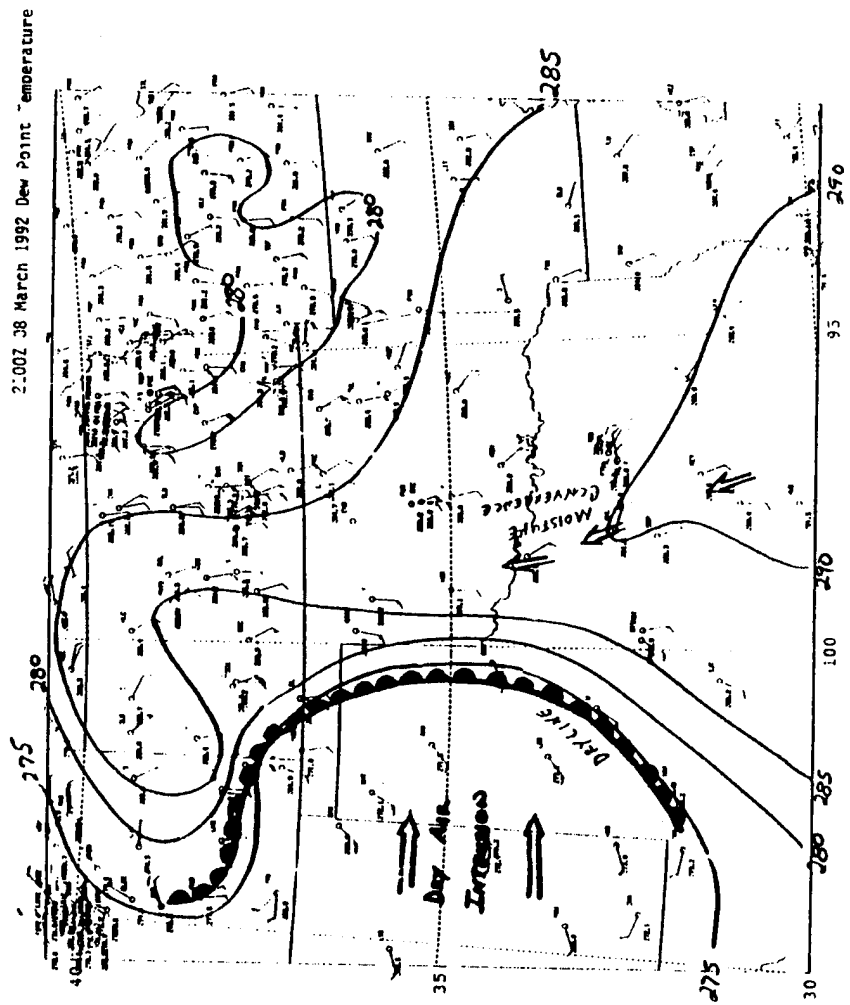


Fig. 6.11. Same as Fig. 6.10, except for 2100Z 08 March 1992.

9-mar-1992,02:01:00 X/Y Wind:c\_windsum.



Fig. 6.12 Sequence of wind profiler observations from Purcell, Ok. Valid time: 2100Z 08 Mar 92 to 0200Z 09 Mar 92. Wind barbs in m/s; Altitude on left: 0m to 4000m.

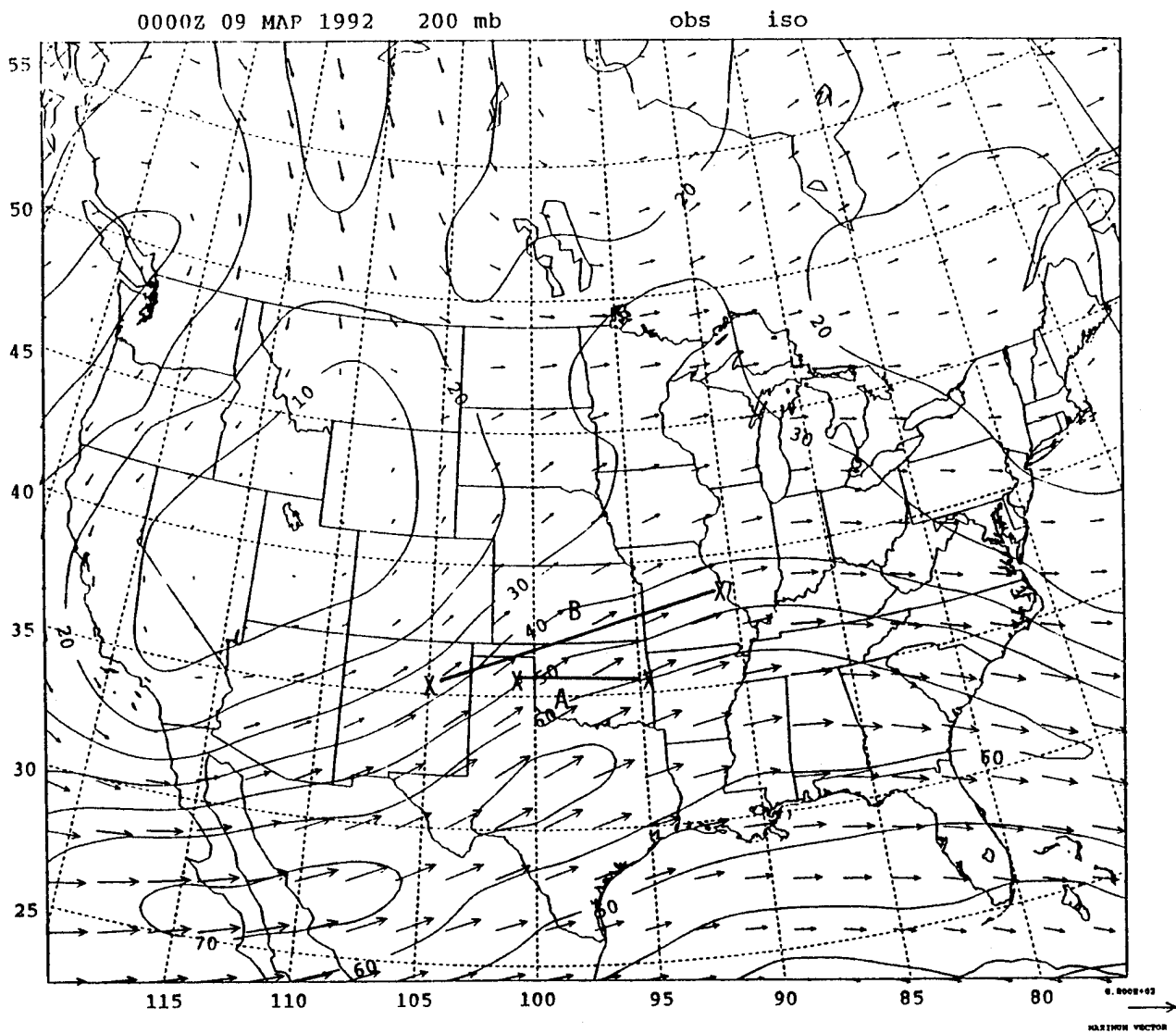


Fig. 6.13. 200 mb isotach analysis with wind vectors, valid at 0000Z 09 March 1992. Note the 70 m/s jet streak over Texas. Cross-section positions noted by 10A and 10B.

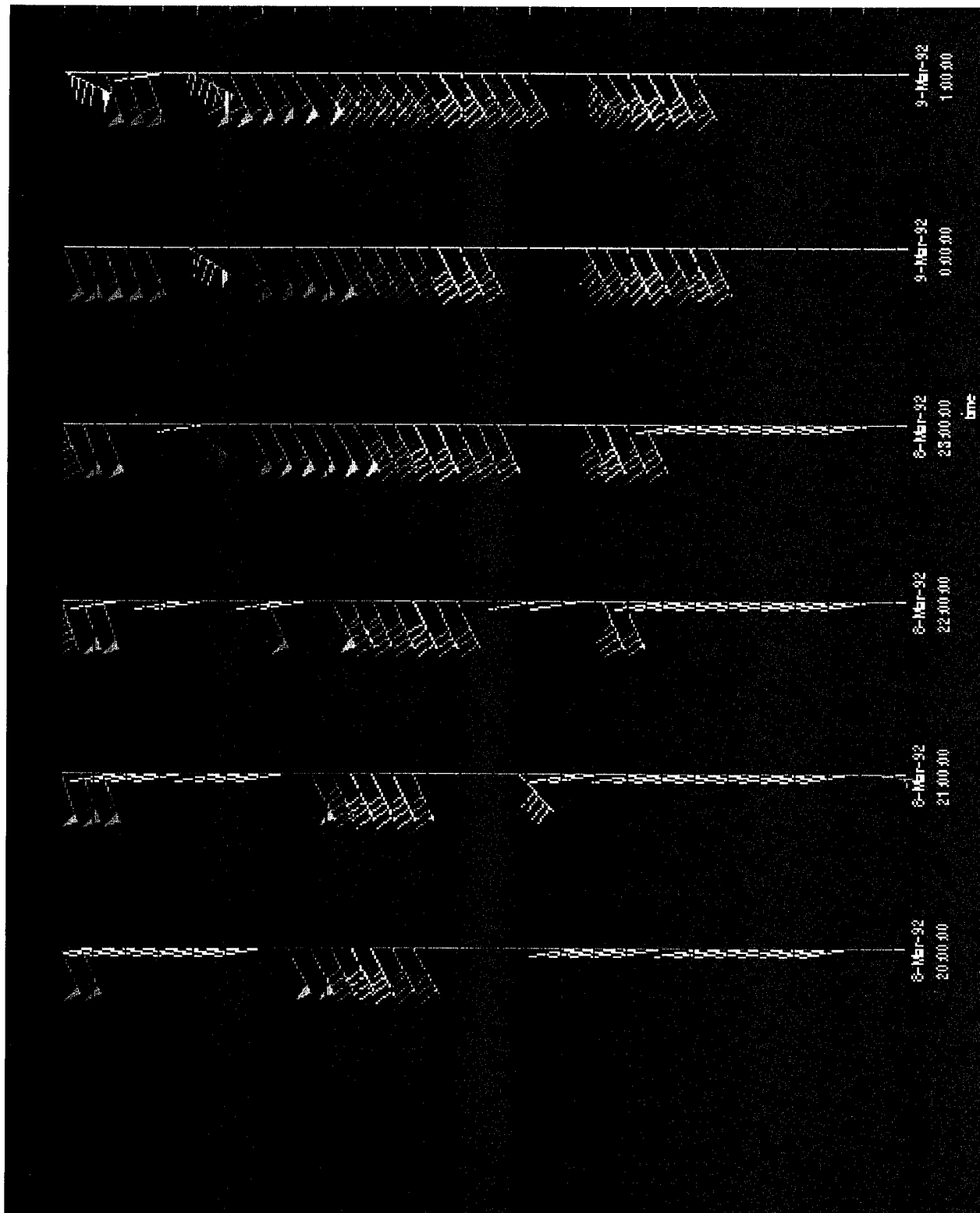


Fig. 6.14. Sequence of wind profiler observations from Purcell, Ok. Valid time: 2000Z 08 Mar 92 to 0100Z 09 Mar 92. Wind barbs in m/s; Altitude on left: 5000m to 15000m.

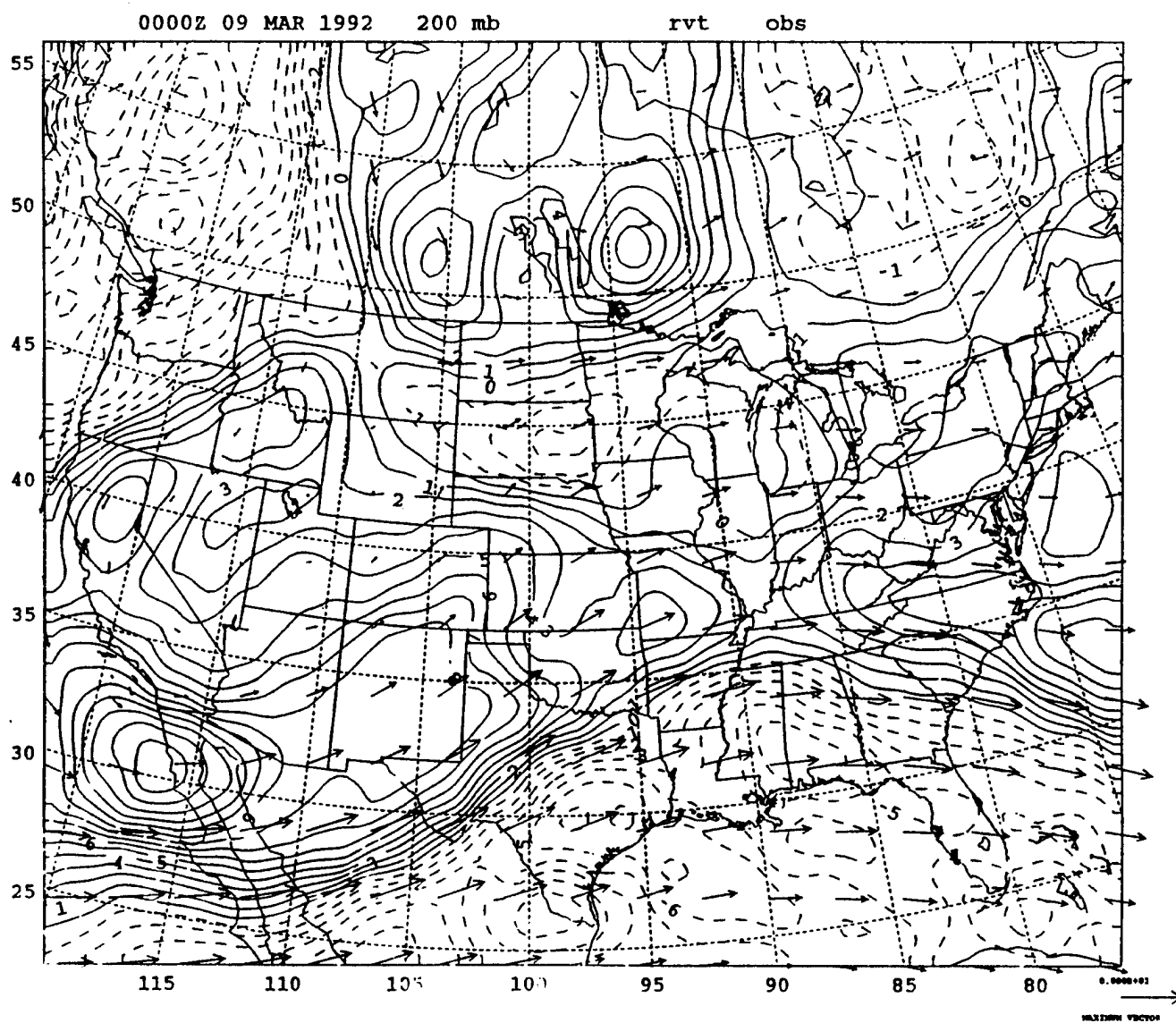


Fig. 6.15. 200 mb relative vorticity for 0000Z 09 March 1992, with 200 mb wind vectors.

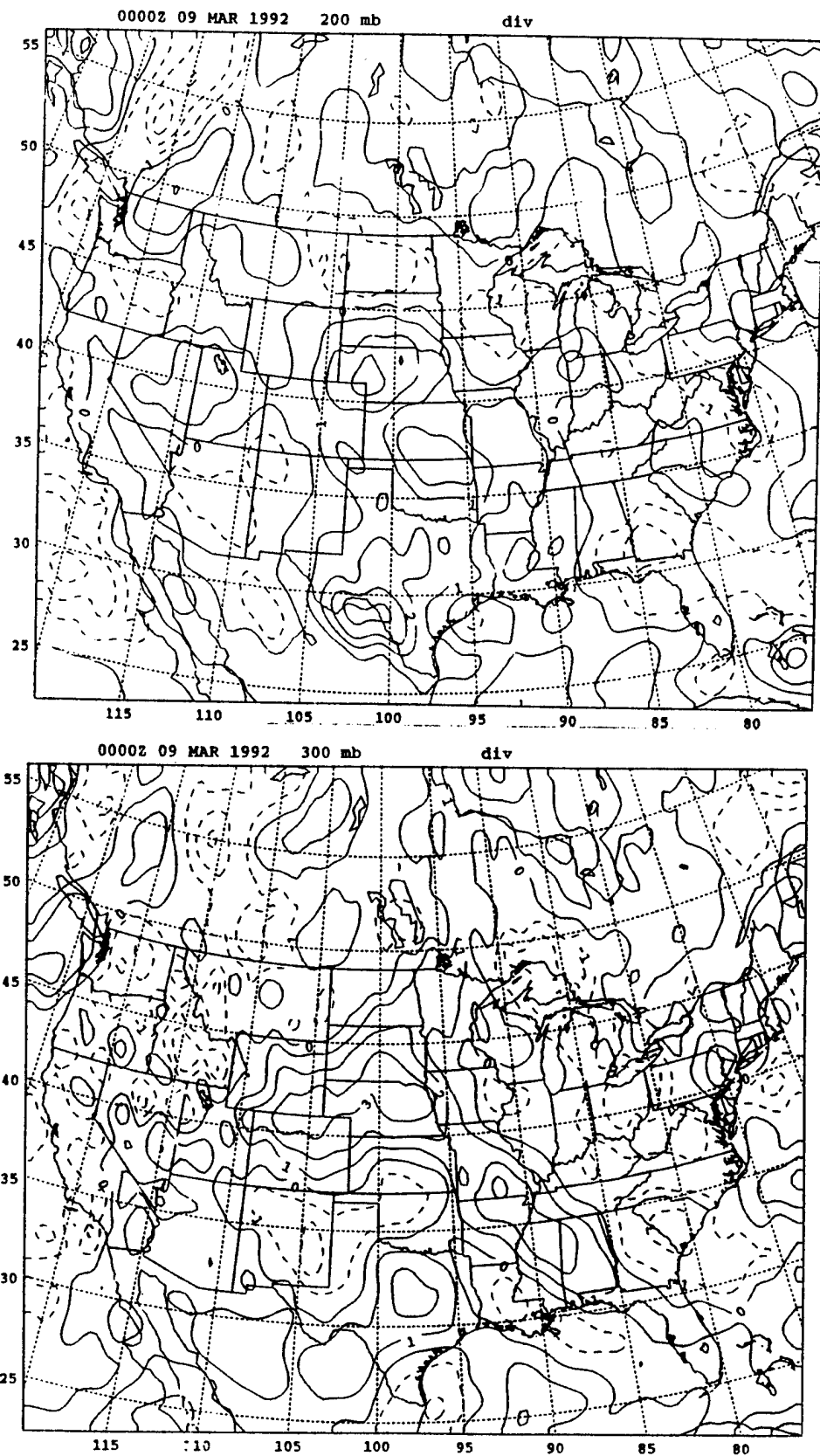
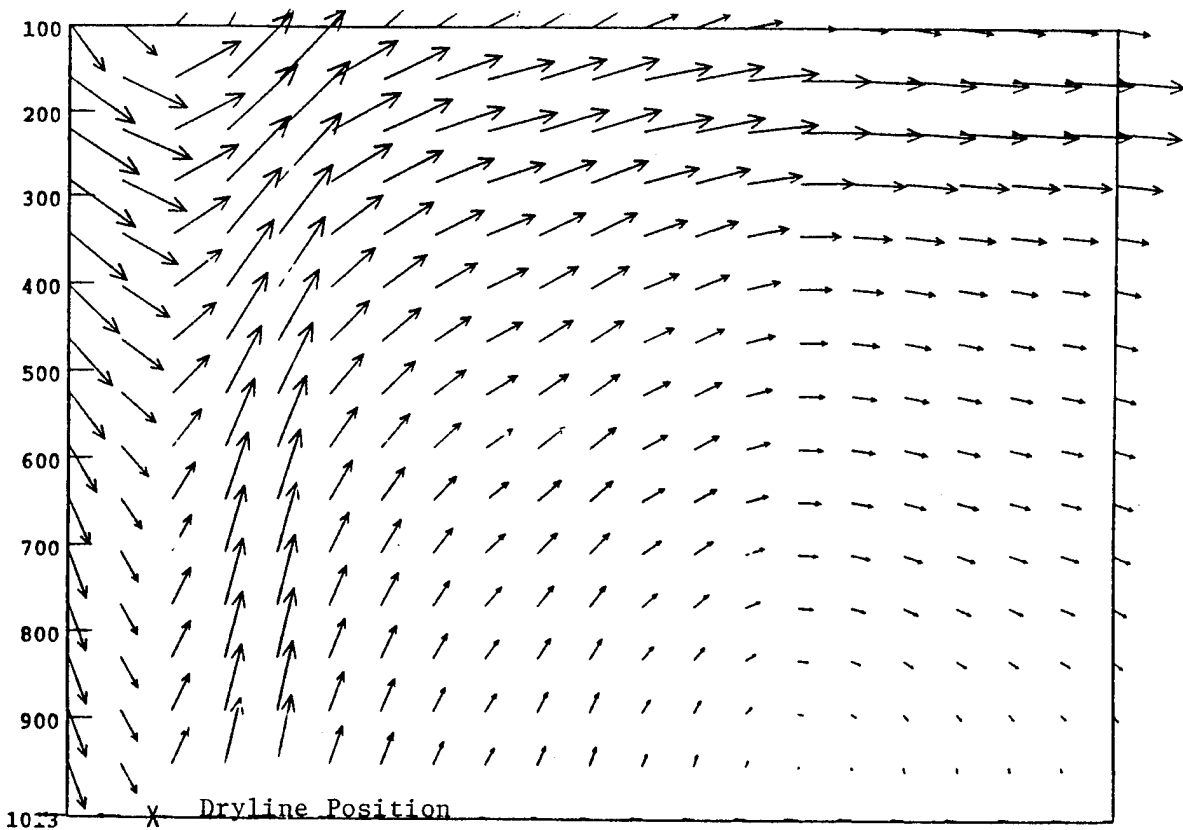


Fig. 6.16. Divergence for (a) 200 mb, and (b) 300 mb.

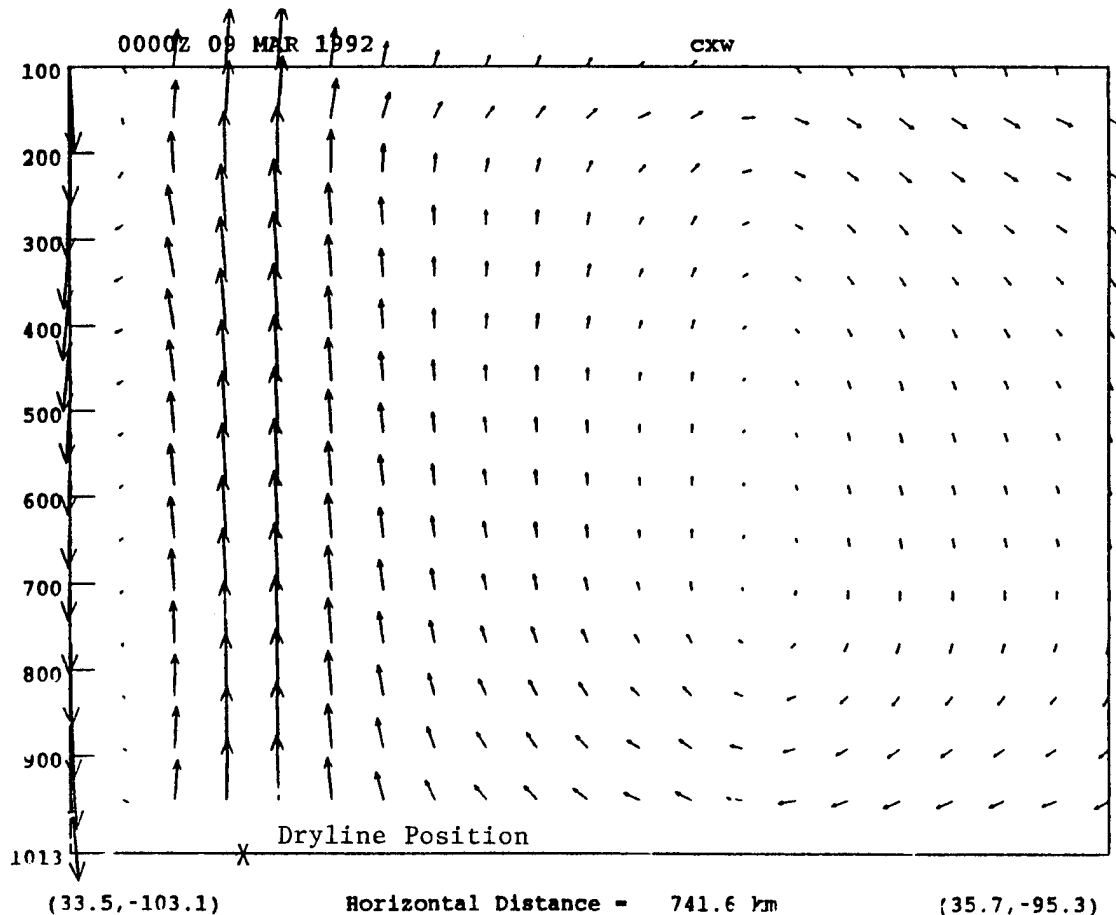


(35.5, -102.7)

Horizontal Distance = 708.7 km

(35.7, -95.3)

0.0002



0000Z 09 MAR 1992

CXW

(33.5, -103.1)

Horizontal Distance = 741.6 km

(35.7, -95.3)

Fig. 6.17. Vertical cross-section across dryline: (a) section 10A, total wind field, and (b) section 10B, ageostrophic wind component only.

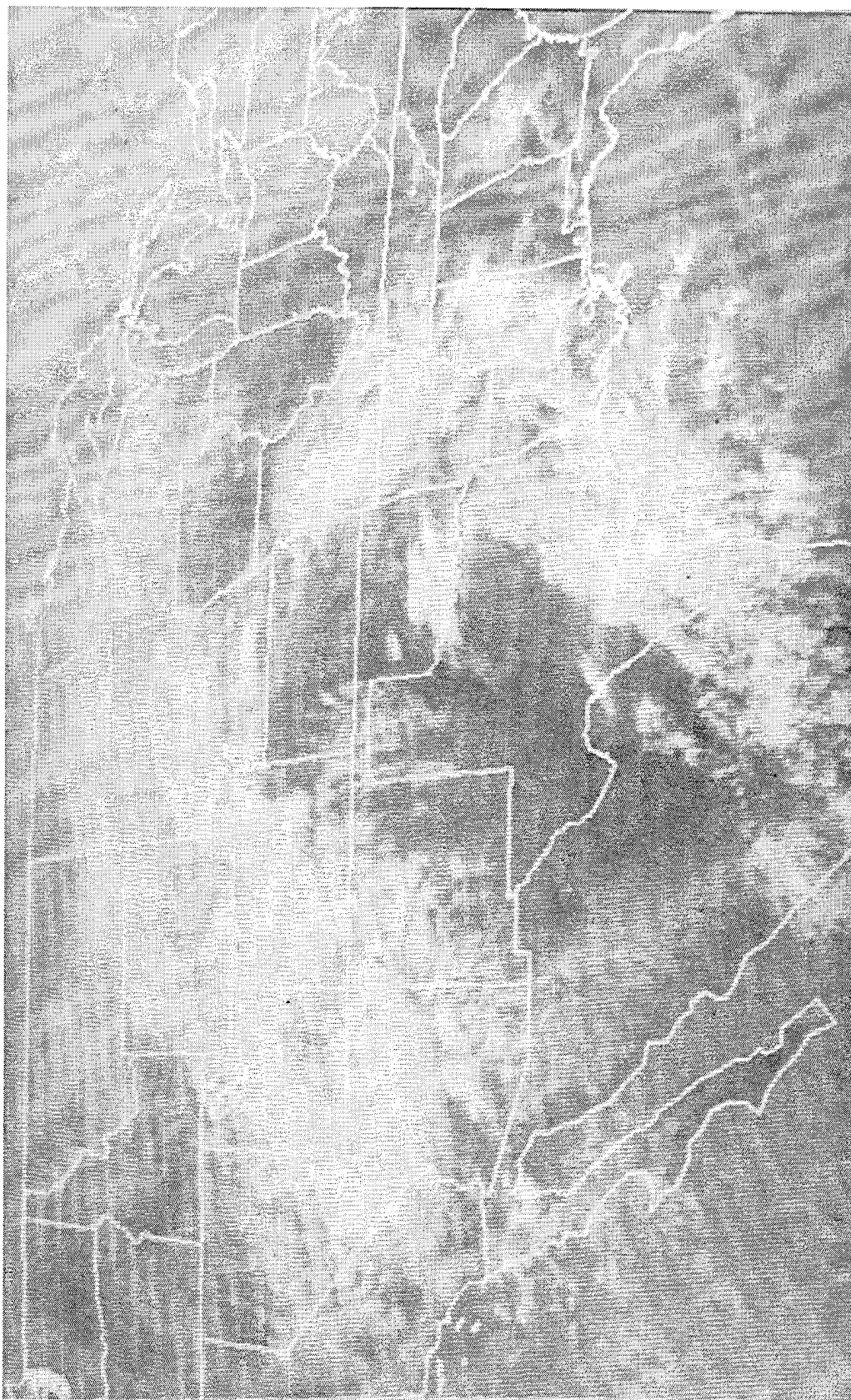


Fig. 6.18. 2300Z 08 Mar 92 GOES infrared image.

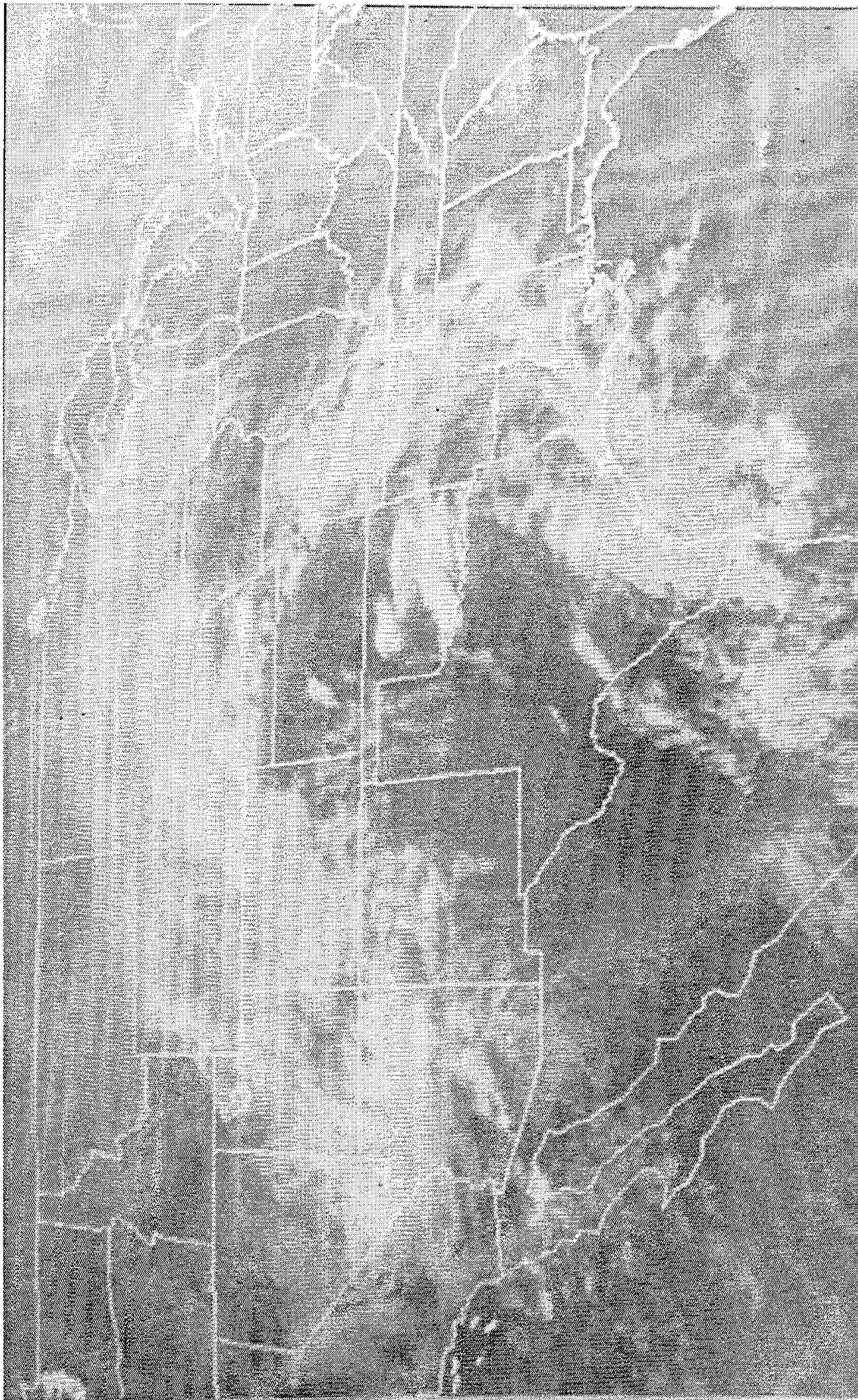


Fig. 6.19. 0000Z 09 Mar 92 GOES infrared image.

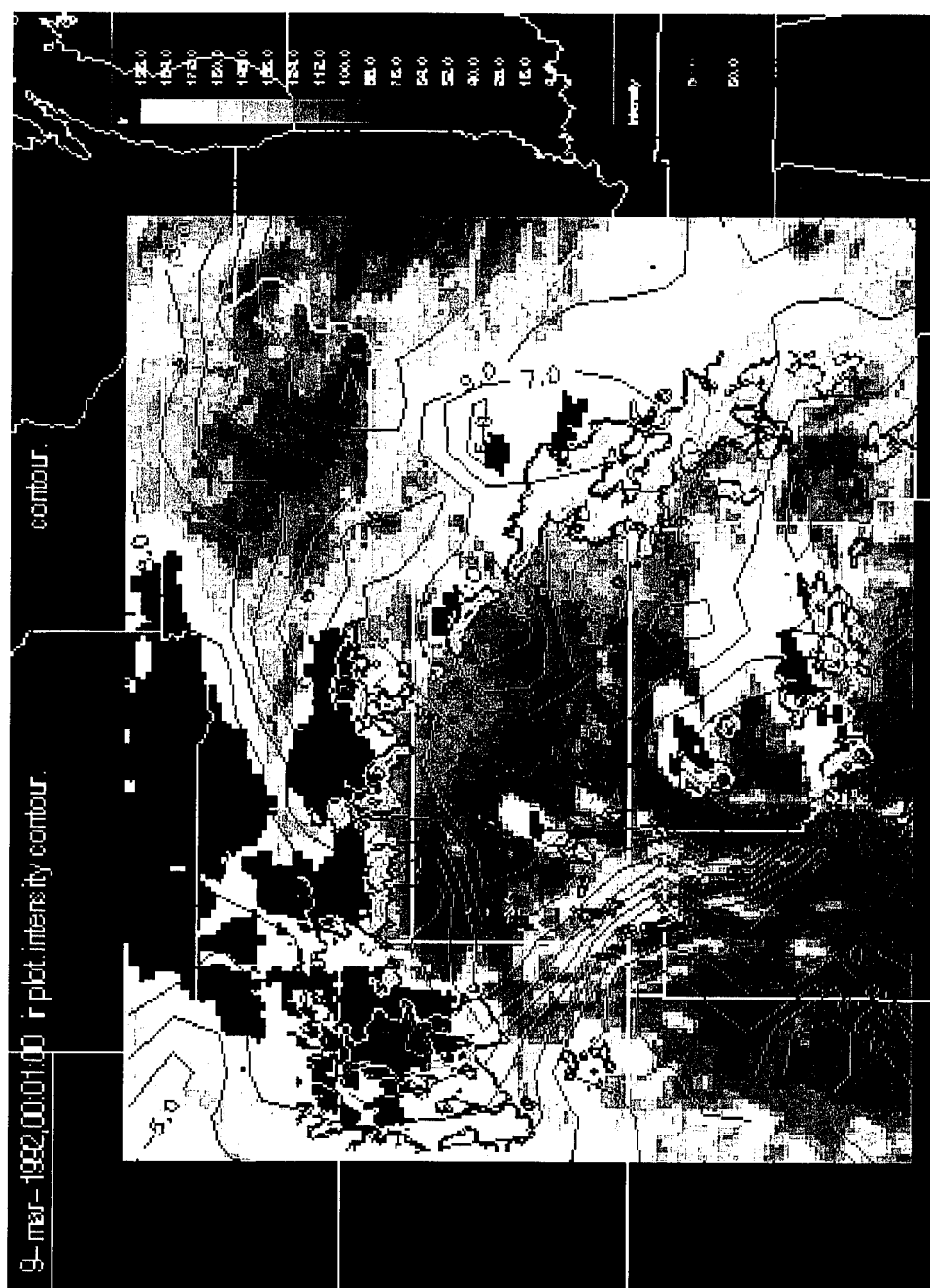


Fig. 6.20. 0001Z 09 Mar 92 GOES enhanced infrared image with composite NWS weather radar reflectivity data and NCAR enhanced data set dew point analysis overlaid.

## VII. CONCLUSION

In Texas and Oklahoma, during the middle afternoon hours, a few convective cells developed along a dryline that extended from Kansas to Big Bend, Texas. On that afternoon, atmospheric mechanisms had evolved to cause those cells to rapidly develop into a severe squall line. This MCS lasted for more than 12 hours and produced five tornadoes, damaging downburst winds, baseball-sized hail and widespread flash flooding.

A complex low pressure system over Colorado that morning (1200Z 08 March 1992) tracked east and deepened. The associated cold front moved across the Texas panhandle during the afternoon and evening hours as an intensifying middle-tropospheric short wave moved rapidly from northern Mexico into Oklahoma during the ensuing 24 hours. The propagation of the short wave caused middle-tropospheric winds to advect dry, warm air northeast from the upper southwest plateau regions of New Mexico and northern Mexico. Schaefer (1986) refers to this as a Mexican plume. A jet streak of 140 to 160 kts developed by 0000Z, 09 March 1992 over central Texas. A low-level jet, identifiable in profiler data, acting in unison with the bulge in the dryline, resulted in increased moisture convergence ahead of the dryline. The combination of the Mexican plume aloft and moisture convergence in the boundary layer resulted in a potentially unstable environment.

A combination of synoptic-scale and mesoscale analysis revealed the physical mechanisms responsible for providing the lifting required to release the potential instability. Meso-analysis has indicated that convection was not initiated until the cold front propagated into the position of the dryline. This would provide mechanical lifting up the frontal surface releasing the convective available potential energy above the level of the inversion. This motion was enhanced by processes related to the 200 mb jet streak and mid-tropospheric short wave. The jet streak and short wave provided lifting by: 1)

positive vorticity advection aloft, and 2) ascent due to a transverse vertical circulation at the left exit of the jet streak.

### **VIII. RECOMMENDATIONS**

The analysis of the coarse resolution NMC GDAS fields identified, to some degree, the short wave and jet streak responsible for much of the lifting involved with MCSs associated with bulging drylines. The cross-section, Fig. 6.17, attests to that rather nicely. This may suggest that a high resolution mesoscale model initialized with this type of data (GDAS) would yield a useful short-term forecast that would enable operational forecasters to predict storms of this type more accurately. Evaluation of model runs with test case data is recommended.



## LIST OF REFERENCES

- Bluestein, H.B., 1986: Fronts and jet streaks: a theoretical perspective. *Mesoscale Meteorology and Forecasting*, P. Ray, Ed., Amer. Meteor. Soc., 173-215.
- Bluestein, H.B. and K.W. Thomas, 1984: Diagnosis of a jet streak in the vicinity of a severe weather outbreak in the Texas Panhandle. *Mon. Wea. Rev.*, **112**, 2499-2520.
- Carlson, T.N., 1991: Mid-Latitude Weather Systems, HarperCollins Academic, N.Y., 406-417.
- Cunning, J.B., and S.F. Williams, 1993: *STORMFEST Operations Summary and Data Inventory*, U. S. Wea. Res. Prog. Off.
- Martin, J.E., J. Locatelli, P. Hobbs, P. Weng and J. Castle, 1995: Structure and evolution of winter cyclones in the central United States and their effects on the distribution of precipitation. Part I: a synoptic-scale rainband associated with a dryline and lee trough. *Mon. Wea. Rev.*, **123**, 241-264.
- McCarthy, J., and S.E. Koch, 1982: The evolution of an Oklahoma dryline. Part I: A meso- and subsynoptic-scale analysis. *J. Atmos. Sci.* **39**, 225-236.
- Rotunno, R., J.B. Klemp and M. Weisman, 1988: A theory for strong, long-lived squall lines. *J. Atmos. Sci.*, **45**, 463-485.
- Schaefer, J.T., 1986: The dryline. *Mesoscale Meteorology and Forecasting*, P. Ray, Ed., Amer. Meteor. Soc., 549-570.
- Weisman, M.L. and J.B. Klemp, 1986: Characteristics of convective storms. *Mesoscale Meteorology and Forecasting*, P. Ray, Ed., Amer. Meteor. Soc., 331-358.
- Weisman, M.L. and J.B. Klemp, 1984: The structure and classification of numerically simulated convective systems in directionally varying wind shears. *Mon. Wea. Rev.*, **112**, 2479-2498.



# **INITIAL DISTRIBUTION LIST**

	No. Copies
1. Defense Technical Information Center Cameron Station Alexandria, Virginia 22304-6145	2
2. Library, Code 52 Naval Postgraduate School Monterey, California 93943-5101	2
3. Chairman, Department of Meteorology Code MR/HY Naval Postgraduate School 589 Dyer Rd Rm 252 Monterey, California 93943-5114	1
4. Prof. W. A. Nuss Code MR/NU Naval Postgraduate School 589 Dyer Rd Rm 252 Monterey, California 93943-5114	1
5. LCDR Raymond Robichaud OA Division USS Independence FPO AP 96618-2760	2
6. Commander Naval Meteorology and Oceanography Command 1020 Balch Boulevard Stennis Space Center, Mississippi 39529-5005	1
7. Commanding Officer FLENUMMETOCCEN 7 Grace Hopper Ave. Stop 4 Monterey, California 93943-5501	1
8. Superintendent Naval Research Laboratory 7 Grace Hopper Ave. Stop 2 Monterey, California 93943-5502	1

- |     |  |   |
|-----|--|---|
| 9.  | Dr. Teddy Holt<br>Naval Research Laboratory<br>7 Grace Hopper Ave. Stop 2<br>Monterey. California 93943-5502 | 1 |
| 10. | Chairman<br>Oceanography Department<br>U.S. Naval Academy<br>Annapolis, Maryland 21402                       | 1 |
| 11. | Chief of Naval Research<br>800 N. Quincy Street<br>Arlington, Virginia 22217                                 | 1 |
| 12. | NOAA Library<br>7600 Sand Point Way NE<br>Building 3<br>Seattle, Washington 98115                            | 1 |
| 13. | Dr. J. R. Bettis<br>1076 Rambling Rd<br>Simi Valley, California 93065  | 2 |